

Aija Närvänen

DED+MACHINING AS AN ALTERNATIVE APPROACH TO TRADITIONAL MANUFACTURING

A feasibility study focusing on production metrics

Master Thesis Work
Faculty of Engineering and
Natural Sciences
Examiner: Hossein Mokhtarian
Examiner: Eric Coatanéa
2025

ABSTRACT

Aija Närvänen: DED + machining as an alternative approach to traditional manufacturing
Master thesis work
Tampere University
Mechanical Engineering
May 2025

WAAM (Wire Arc Additive Manufacturing) is an additive manufacturing method evolved from traditional welding technology. It has recently drawn attention due to its capability of manufacturing components with high manufacturing efficiency and low production cost. WAAM has high deposition rate and high heat input which makes the production fast. However, those also contribute to some of WAAM manufacturing key challenges, high surface roughness, geometrical distortion and large feature size. To improve these issues WAAM is often combined with machining to achieve both effective production and high surface quality. Though, combining these two manufacturing methods has proven challenging. Furthermore, there is little to no information to support full utilization of WAAM + machining manufacturing in industrial production.

The objective of this thesis was to investigate WAAM + machining manufacturing method as an alternative to manufacturing approach for fully machined component. A literature review and investigation through two case studies was performed. WAAM + machining was found to be a promising alternative to traditional manufacturing. By utilizing hybrid WAAM + machining manufacturing machining time and machining length could be reduced. However, when comparing the case study results to literature machining was found to be more effective and ecological manufacturing method. By applying primitive geometries in the redesign phase, the production process was simplified. Furthermore, complex features could be fabricated through effortless and uncomplicated manufacturing process. WAAM + machining is a serious competitor to traditional manufacturing methods, and it deserves to be adapted to be a part of everyday design and manufacturing.

Keywords: WAAM, arc-DED, hybrid WAAM manufacturing, WAAM + machining

The originality of this thesis has been verified using the Turnitin Originality Check service.

TIIVISTELMÄ

Aija Närvänen: DED + machining as an alternative approach to traditional manufacturing
Diplomityö
Tampereen yliopisto
Konetekniikan diplomi-insinööri
Toukokuu 2025

WAAM (Wire Arc Additive Manufacturing) on perinteisestä hitsaustekniikasta kehittynyt materiaalia lisäävä valmistusmenetelmä. Se on viime aikoina herättänyt huomiota, sillä sen avulla voi valmistaa osia tehokkaasti alhaisilla tuotantokustannuksilla. WAAM valmistusmenetelmällä on suuri materiaalinsyöttötahti ja sekä suuri lämmöntuonti, mikä tekee sen tuotantotahdista nopean. Nämä kuitenkin osaltaan edistävät valmistusmenetelmän suurimpia haasteita, joita ovat korkea pinnankarheus, geometrinen vääristymä sekä suuri piirre koko. Näiden haasteiden ratkaisemiseksi WAAM yhdistetään usein koneistukseen, jolloin saavutetaan sekä tehokas valmistustahti että korkea pinnanlaatu. Näiden kahden valmistusmenetelmän yhdistäminen on osoittautunut haastavaksi. Lisäksi saatavilla on vain vähän tai ei lainkaan tietoa, joka tukisi WAAM + koneistus -valmistusmenetelmän täydellistä hyödyntämistä teollisessa tuotannossa.

Tämän opinnäytetyön tavoitteena oli tutkia WAAM + koneistus -valmistusmenetelmää ja tukea sen käyttöönottoa teollisuuden tuotannossa. Aihetta tutkittiin kirjallisuuskatsauksella sekä kahden tapaustutkimuksen kautta. WAAM + koneistuksen todettiin olevan lupaava vaihtoehto perinteiselle valmistukselle. WAAM + koneistus valmistuksella voitiin lyhentää koneistusaikaa sekä koneistuspituutta. Tapaustutkimuksen tuloksia verrattaessa kirjallisuuteen todettiin koneistuksen kuitenkin olevan tehokkaampi ja ekologisempi vaihtoehto. Hyödyntämällä primitiivisiä geometrioita tuotantoprosessia pystyttiin yksinkertaistamaan, ja monimutkaisia geometrioita voitiin valmistaa vaivattomasti. WAAM + koneistus on varteenotettava kilpailija perinteisille valmistusmenetelmille, ja se ansaitsee tulla mukautetuksi osaksi jokapäiväistä suunnittelua ja valmistusta.

Avainsanat: WAAM, arc-DED, hybridi WAAM valmistus, WAAM + koneistus

Tämän julkaisun alkuperäisyys on tarkastettu Turnitin Originality Check -ohjelmalla.

USE OF AI IN THESIS

I have utilised AI tools in my thesis:

- No
- Yes

I acknowledge that I am fully responsible for the entire content of my thesis, including the parts generated by AI, and accept accountability for any violations of ethical standards in publications.

PREFACE

This mechanical engineering student has overcome several obstacles whilst pursuing engineering degree. However, none so demanding and challenging yet highly interesting as researching and writing this thesis. Without assistance and support this thesis would not be, and I appreciate every one of you who helped me directly or indirectly. Thank you.

Tampere, 30 May 2025

Aija

CONTENTS

1.INTRODUCTION	1
2.THEORETICAL BACKGROUND.....	4
2.1 WIRE ARC ADDITIVE MANUFACTURING	4
2.2 WAAM COMPONENTS AND PART GEOMETRY	6
2.2.1 Characteristics of WAAM components	7
2.2.2 Build up and path planning.....	10
2.2.3 Component geometry and characteristics	13
2.2.4 Traditional manufacturing of engine housing	16
2.3 WAAM manufacturing process	18
2.3.1 Process parameters.....	19
2.3.2 Process flow/steps	21
2.4 POST-PROCESS MACHINING	22
2.4.1 System setups and process strategies.....	23
2.4.2 Considerations of design.....	23
2.4.3 Machining WAAM component.....	24
2.5 PROCESS AND COMPONENT EVALUATIONS	25
2.5.1 Economic analysis	25
2.5.2 Sustainability analysis.....	26
2.5.3 Productivity analysis	28
3.RESEACH METHODS AND MATERIALS	29
3.1 Methodological approach overview.....	29
3.2 Investigating process parameters	30
3.2.1 Single weld bead investigation	31
3.2.2 Overlapping parameter investigation.....	32
3.2.3 Weaving or oscillating	34
3.3 Creating case study geometries	35
3.3.1 Case study 1 geometry	36
3.3.2 Case study 2 geometry	38
4.RESULTS AND THEIR REVIEW	43
4.1 Manufacturing case study 1	43
4.1.1 Deposition of case study 1	43
4.1.2 Form fault measurement.....	44
4.1.3 Component scan and machining simulation	46
4.1.4 Machining post-processing	49
4.1.5 Evaluation of case 1.....	51
4.2 Manufacturing case study 2.....	54
4.2.1 Deposition of case study 2.....	54
4.2.2 Component scan and machining simulation	56
4.2.3 Evaluation of case study 2	59
5.SUMMARY AND CONCLUSIONS	62
REFERENCES.....	64

LIST OF FIGURES

Figure 1. History and development of WAAM [3].....	1
Table 1. Features and values of WAAM [11].....	4
Figure 2. A map of different metal additive manufacturing processes, adapted from [13].....	5
Table 2. Comparison of different WAAM processes based on type of energy source [14], [15].	6
Figure 3. Different methods for utilizing substrate in WAAM, adapted from [12].	8
Figure 4. Most common materials in relation to typical defects [15].....	9
Figure 5. Cross-section of bead layer, adapted from [28].	11
Figure 6. General filling paths, adapted from [26].	12
Figure 7. Parallel deposition path compared to weaving (oscillating) deposition path [32].	13
Figure 8. Nature inspired 2,5D geometry parts [16].	14
Figure 9. Demonstration part of WAAMs capability to produce different geometries and features [40].	15
Figure 10. Demonstration part containing different deposition paths and multiple cross sections [33].	16
Figure 11. WAAM process parameters [49].	19
Figure 12. Flow chart of different production phases in WAAM manufacturing process.	22
Figure 13. Production processes of WAAM and machining manufacturing technologies.	27
Figure 14. Chosen methodology approach.	29
Figure 15. Demonstration of used setup at Tampere University.	30
Table 3. Composition of welding wire [67].	31
Table 4. Investigating process parameters.	31
Figure 16. Produced wall specimens with different process parameters (trade-off between printing time and quality).	32
Figure 17. Cross-section of bead layer to clarify values in equation (1) [26].	32
Figure 18. Three overlapping walls produced with (a) 8% CO ₂ and 92 % Ar, 37,5% overlap, (b) 2% CO ₂ and 98 % Ar, 40% overlap, (c) 18% CO ₂ and 82 % Ar, 35% overlap.	33
Figure 19. Weaving path and required main parameters, adapted from [34]	34
Figure 20. Results of circular path testing: (a) two bead overlapping deposition, (b) weaving deposition, (c) side profile comparison of overlapping (left) and weaving (right).	35
Figure 21. Geometry of case 1: Cycloid drive housing.	36
Figure 22. Case 2 final designed geometry.	39
Figure 23. Case 2 redesigned geometry.	40
Figure 24. Planned path for first build up (left) and for the whole first build-up.	42
Figure 25. Calibration and result of deposited component.	44
Table 5. WAAM deposition values for case study 1.	44
Figure 26. Defined measurement points, (a) 28 points for plane 1 and (b) 18 points for plane 2 and (c) measured components.	45
Table 6. Results of form fault measurements.	46
Figure 27. Wall thickness assessment, in which red colour indicates the areas below limit value.	47
Figure 28. Deposited part as stock model (red colour: final model, grey colour: deposited model, greenish colour: extra deposited material including material allowance).	48

<i>Figure 29. Comparison of material losses for two different inputs in machining simulation (left: Cylindrical raw stock, right: WAAM deposited component).....</i>	<i>48</i>
<i>Table 7. Post-processing values of deposited and traditional block raw stocks in case study 1.....</i>	<i>49</i>
<i>Figure 30. WAAM + machining result of P3 case 1.</i>	<i>50</i>
<i>Figure 31. WAAM + machining result of P2 component.</i>	<i>50</i>
<i>Figure 32. A Graph of case 1 production efficiency of different manufacturing methods.</i>	<i>52</i>
<i>Figure 33. Cost structure of case study 1, total cost: 44 €.</i>	<i>52</i>
<i>Figure 34. Cost per unit in relation to production volume [64].</i>	<i>53</i>
<i>Table 8. Illustration of different layer deposition times (deposition time decreases due to lessened feature deposition as layers increase).</i>	<i>54</i>
<i>Figure 35. Result of deposition of case study 2.....</i>	<i>55</i>
<i>Figure 36. Scanned deposition geometry and comparison with primitive shape geometry model.</i>	<i>56</i>
<i>Figure 37. Successive scanned deposition model and final geometry model (red colour: final model, grey colour: deposited model, greenish colour: extra deposited material including material allowance).....</i>	<i>57</i>
<i>Figure 38. Three cross-section view of deposited features.</i>	<i>58</i>
<i>Figure 39. Comparing different material losses and different raw stocks in machining simulation (left: block raw stock, right: WAAM deposited raw stock).</i>	<i>59</i>
<i>Table 9. Post-process machining values for deposited and traditional raw stock models in case study 2.....</i>	<i>59</i>
<i>Table 10. Comparing true and estimated layer heights.</i>	<i>60</i>

LIST OF SYMBOLS AND ABBREVIATIONS

AM	Additive Manufacturing
CAD	Computer Aided Design
CAM	Computer Aided Manufacturing
CMT	Cold Metal Transfer
CNC	Computerized Numerical Control
DED	Direct Energy Deposition
GMAW	GAS Metal Arc Welding
GTAW	Gas Tungsten Arc Welding
LCA	Life Cycle Assessment
LCC	Life Cycle Costing
PAW	Plasma Arc Welding
TCMAW	Tandem Gas Metal Arc Welding
WAAM	Wire Arc Additive Manufacturing
2,5D	2,5 -dimensional
3D	3 -dimensional

1. INTRODUCTION

WAAM is a modern additive manufacturing process for metals. It uses arc as a heat source and falls under the category of Direct Energy Deposition (DED). It is said to be evolved from traditional welding technology. [1] WAAM as manufacturing method has been studied for over thirty years, however the first patent dates back to 1925 [2]. The development of WAAM is elaborated in Figure 1.

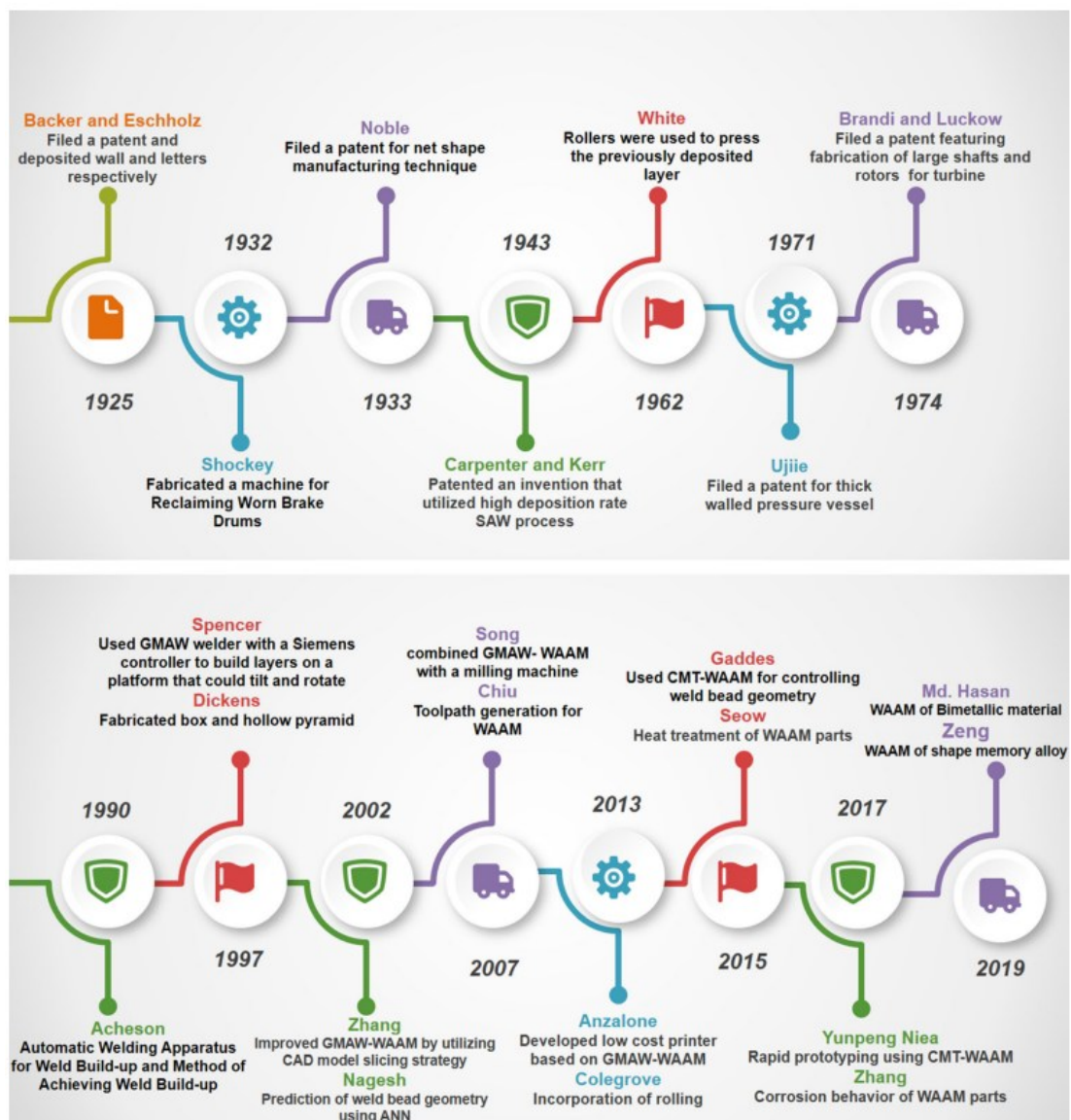


Figure 1. History and development of WAAM [3].

WAAM has recently gained more attraction among all Additive Manufacturing (AM) technologies due to its great potential. It can fabricate medium-to-large-scale structures with low production cost and high manufacturing efficiency. These components are often solid and can be up to tens of meters long. [4] WAAM components have good structural integrity and a range of materials from titanium to steel and aluminum can be utilized in production. Most common way to manufacture WAAM components is to produce near-net-shape structures. WAAM is a serious competitor for traditional subtractive manufacturing methods due to its ability to produce valuable structural parts with reduced cost and material losses in shorter times. [5]

High deposition rate and high heat input makes WAAM production fast. However, it also contributes to one of the most prominent challenges of WAAM components, high surface roughness. To combat this challenge WAAM manufacturing is often followed by post-process machining. Combined WAAM + machining can produce components fast with great material savings as well as achieve the roughness and geometrical precision commonly found in machined components. Though, performing WAAM + machining hybrid operation has proven challenging. [6]

There is still much to investigate in combined WAAM + machining manufacturing method. Furthermore, there is an information gap from manufacturing investigation to fully utilizing WAAM + machining advantages in component production. This thesis focuses on this subject area, focusing on 2,5 -dimensional (2,5D) components. The main question to be answered is: How can WAAM, particularly in combination with subtractive machining, be utilized to manufacture near-net-shape geometry of 2.5-dimension components as an alternative to fully machined components? Furthermore, this leading question is then refined with the following supporting research questions:

1. What are the characteristics, advantages, limitations and key challenges of integrating WAAM with subtractive machining processes?
2. How are WAAM components manufactured?
3. Which types of components or industries could benefit from adopting a WAAM + Machining process?

The structure of the thesis proceeds accordingly. In section two a literature review is conducted to learn theoretical background of WAAM and hybrid WAAM + machining manufacturing methods. Section three and four implements foregoing theory by overseeing production of two case studies. In the first case study we investigate simple cycloid drive housing geometry and in the second case study more complex 2,5D geometry

is investigated. Lastly, in section five the results of two case studies are reviewed, further conclusion drawn and compared to existing literature.

2. THEORETICAL BACKGROUND

2.1 WIRE ARC ADDITIVE MANUFACTURING

Wire arc additive manufacturing (WAAM) is a process where metal wire or metal powder is fed directly into a melt pool caused by electron beam or a laser [7]. DED processes can use either arc, e-beam or laser as a heat source and often operates with shielding gas flux over melted surface but can also work in an inert atmosphere [1]. Variety of metals can be used in this process, such as stainless steel, tool steel, nickel, titanium, cobalt and aluminum alloys [8], [9]. In this thesis we are focusing on WAAM, which is one of the DED processes. WAAM uses an electric arc heat source and metal wire as a feed stock [10]. On the Table 1 below are some general feature values of WAAM process and end results:

Table 1. Features and values of WAAM [11].

Layer thickness (μm)	Deposition rate (g/min)	Dimensional accuracy (mm)	Surface roughness (μm)
~1500	12	±0.2	200

WAAM setup contains two main modules: the motion module and deposition module. The latter creates the deposition process and the former controls the movement of the carrier head and deposition, thus determining the geometry of the object. Main setups can be divided into two categories, robotic and Computer Numerical Control (CNC) based setup. [12] Generally robotic based setup is more common [7].

WAAM is one method for printing metal, but there are several other methods as well. From Figure 2 you can see a map summary of different methods in relation to each other. Compared to other metal additive manufacturing techniques, WAAM can produce large and complex-shaped parts relatively fast [10]. Additionally, because the wire feed stock is deposited layer-by-layer into the part, WAAM has high efficiency on material usage, even up to 100 %. This makes it more environmentally friendly technique, in addition to the fact it does not include risky powder environment. Furthermore, metal wires are more cost effective, easier available and have lower cost compared to metal powders suitable for additive manufacturing processes. [11] With WAAM metal can also be laid on complex and nonplanar surfaces and the material or purity can be changed within the part

(varying in different layers or slowly change as part is forming), which offers new opportunities for designing. [7] On the other hand, WAAM can entail considerable distortions and residual stresses due to high deposition rate and heat input [11]. Other additive manufacturing techniques might result in better surface finish and better precision [7].

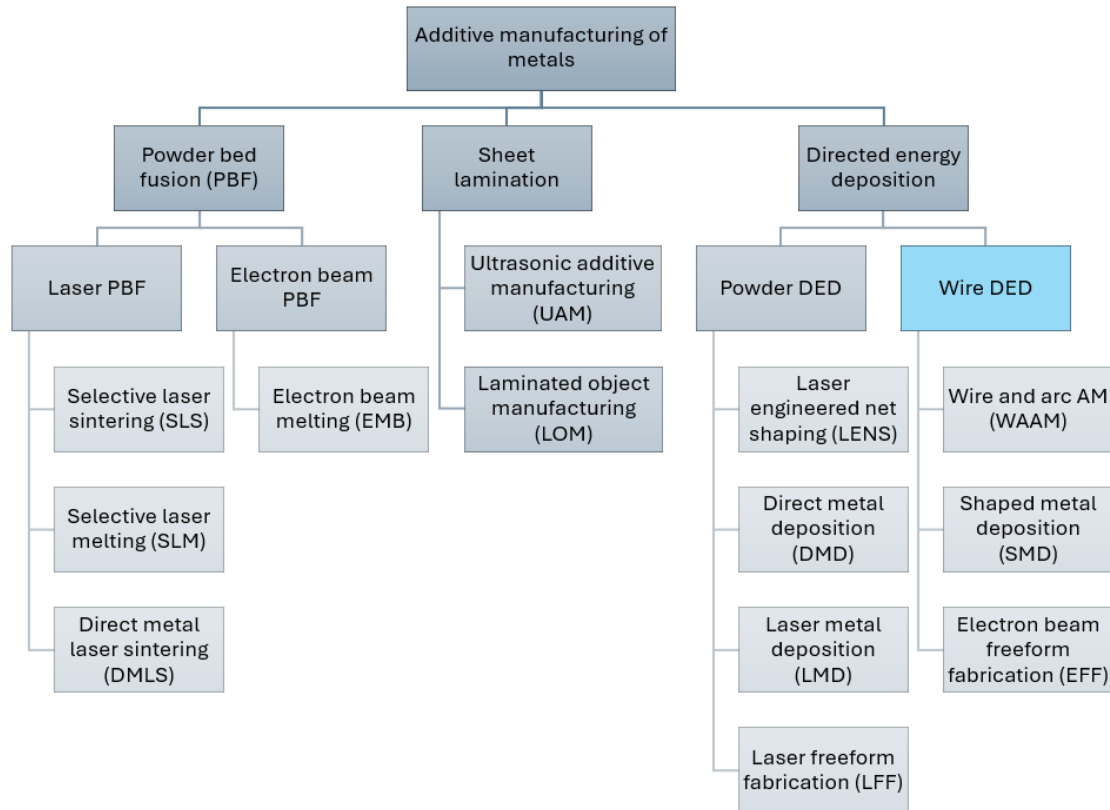


Figure 2. A map of different metal additive manufacturing processes, adapted from [13].

To improve the quality of WAAM components different post-processing treatments are applied. Machining is used to achieve better surface quality, accuracy and enable surface functionality for the part manufactured with WAAM. Other post-processing treatment is heat treatment, which can be used to enhance the mechanical properties of the part and reduce the residual stresses. [4]

A variety of different WAAM system designs have been developed to operate for different levels of production or for different technical requirements. Most usual variations are based on gas metal arc welding (GMAW) and gas tungsten arc welding (GTAW), and a bit less common are tandem gas metal arc welding (TCMAW), cold metal transfer (CMT) (both are variations of GMAW) and plasma arc welding (PAW). [14] Table 2 shows the basic characteristics of different system designs.

Table 2. Comparison of different WAAM processes based on type of energy source [14], [15].

Energy source	Process characteristics	Deposition rate
GTAW	Electrode: non-consumable, wire feed: separate, rotation of torch required	1-2 kg/h
GMAW	Electrode: consumable, poor arc stability, spatter	3-4 kg/h
CMT	Electrode: consumable, heat input: low, dimensional accuracy: high, little to no spatter, high process tolerance	2-3 kg/h
TCMAW	Electrode: two consumable wires, material mixing: easy	6-8 kg/h
PAW	Electrode: non-consumable, wire feed: separate, rotation of torch required	2-4 kg/h

Mechanical properties of WAAM components are in most cases comparable to their traditionally manufactured counterparts. There are some inherent flaws with WAAM such as residual stresses or porosity that can negatively affect the mechanical properties of the component. Furthermore, since WAAM is inherently unbalanced thermal process, formulated microstructure is challenging to predict or control and therefore the produced structures might have a varying mechanical properties. [15]

WAAM is used for producing different metallic, medium-to-large-scale structures/components for multiple industries. Automotive, aerospace and shipbuilding industries are one example, but there is plenty more. WAAM is also commonly used to maintain and repair a damaged components and parts. [4]

2.2 WAAM COMPONENTS AND PART GEOMETRY

WAAM can open a broad range of new design opportunities, with its advantages and disadvantages. WAAM component fabrication involves certain aspects, such as build up orientation, build sequence and strategies, utilization of substrate and certain geometrical constrains. [5] For example, 2,5D geometries can be produced with great efficiency using WAAM [16]. But in some cases, more traditional manufacturing methods might be a better choice.

2.2.1 Characteristics of WAAM components

As in additive manufacturing in general, WAAM component design has inherent design freedoms. Complex shapes can be achieved, and either solid structures, thin-walled elements or combination of both can be constructed. WAAM components vary from small joints and connectors with grid shell structures to solid bridges. [17] The advantages of WAAM include high material utilization and deposition rate, ability to construct complex and large parts with lower cost while maintaining good mechanical properties, and simplification of production process [18], [19]. However, there are some limitations to designing WAAM components as well. The geometry of the structure cannot have significant overhang or projection without support, without the risk of drooping or fall of the melted metal [7]. Thus, minimum allowance for self-supporting angle must be considered. Moreover, both maximum feature size (risk to distortions and residual stresses increase with the size of the component) and minimum feature (welding nozzle size) must be reckoned with. [17] Finally, the process parameters have great influence on the result and can alter the mechanical or geometrical features of the component [19].

With WAAM there is an opportunity to utilize the substrate as part of the final component. Generally, the AM product consists only of the printed part, and the substrate is removed after deposition. But in some cases the substrate can be included in the final product [20]. Different strategies can be applied by utilizing the substrate, and they are presented in Figure 3. Printing can be carried out on one or both sides of the substrate (if substrate can be flipped), and the substrate might be embedded to the final product or be possibly reused for different components. Embedding the substrate in the desired component can save time as fewer layers have to be printed and separation time of part and substrate can be eliminated. Furthermore, some overhang features can be prevented and overall accuracy improved. [12] However, if the deposited part is to be machined, the substrate must as well, to prevent the misalignment of the relative positioning of the printed part and substrate [20].

If substrate is to be flipped to allow deposition on both sides, a symmetrical deposition strategy is recommended. This means, that the substrate is considered as a symmetry plane for the part, and whilst deposition, in between two layers the substrate flips, and material is printed uniformly on both sides. This balances the effects of the significant heat input and reduces residual stresses and distortions. [5]

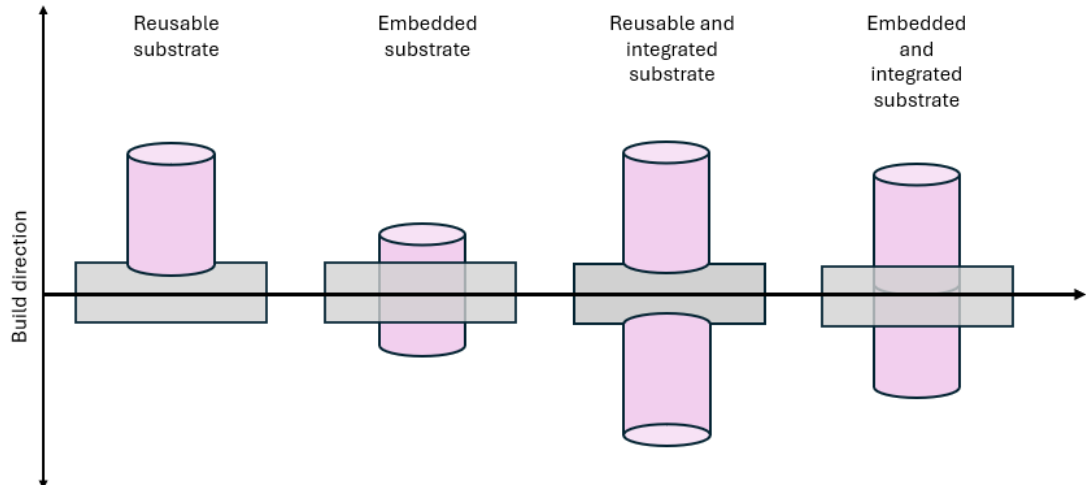


Figure 3. Different methods for utilizing substrate in WAAM, adapted from [12].

The built orientation of the part relative to substrate and nozzle must also be considered. Generally, there are two different build orientations that are used: vertically built (most common) or horizontally built (challenges with thermal gradients, residual stresses and removal of substrate materials) [21].

Unfortunately, there are also some drawbacks to this manufacturing technique that needs to be taken into consideration in the design phase. Parts manufactured with WAAM have rough and wavy surface, and prone to geometric imperfections and distortions due to the high heat accumulation. Therefore, unlike more traditionally produced metal components, WAAM components might have unpredictable geometry and thickness. [17], [19] Moreover, the geometry of deposition beads varies depending on process parameters and welding conditions, which increases the unpredictability of the outcome [10].

Different factors influence the occurrence of imperfections and distortions in WAAM components. Path planning, interlayer temperature and the type of shielding gas, for example, are among these factors. Furthermore, the choice of the choice of material affects the occurrence of imperfections and distortions, since some materials are more susceptible to certain types of defects [15]. Figure 4 compares the material-specific defects for five material categories (Titanium, Aluminum, Steel, Nickel Alloy, and Binetal) in WAAM. The severity of each defect is rated on a scale of one to five.

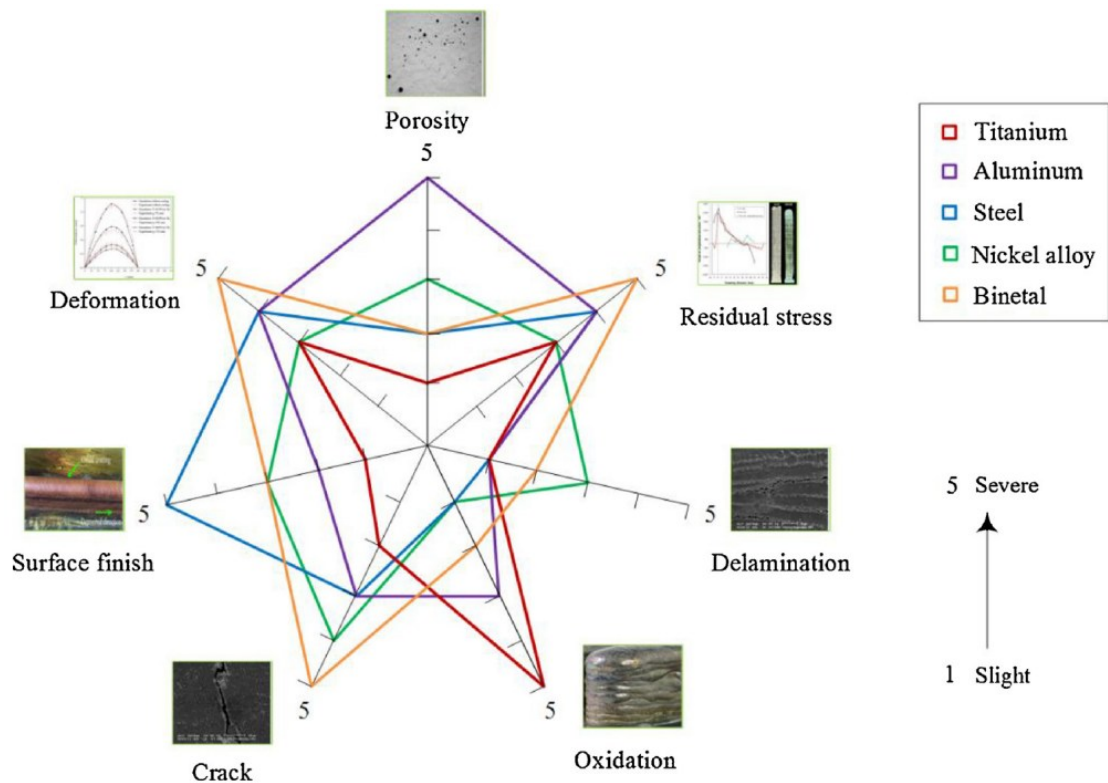


Figure 4. Most common materials in relation to typical defects [15].

One of the major concerns of WAAM process is the control of distortions and residual stresses, which influence the part geometry, and at worst can lead to structures premature failure. Distortions and residual stress are due to thermally induced strains from the non-uniform contraction and expansion of the metal under the influence of heat input. Arising strains may cause the structure to distort during deposition. Sometimes the component is secured thoroughly on all sides and therefore cannot move. Thus, the strains remain locked inside as residual stresses. After unclamping residual stresses will start to distort the component. Alternatively, the strains might cause microscopic failures such as yield or cracks. Even though post-processing can help minimizing residual stress, the best way of limiting both distortions and residual stresses is control them during the build-up. Many techniques have been developed to tackle this issue, considering deposition patterns, sequences or temperature control such as interlayer cooling or preheating. [11]

Since WAAM is basically deposition of parabola-similar curves on top of another, resulting deposited surface has always high surface roughness [11]. Process parameters greatly affect surface roughness, as well as deposition strategy and overhang angles. Two main causes of the surface roughness are the “stair step effect” and “balling”. Fortunately, surface roughness has a small effect on overall stability of the component, especially with larger components. Nonetheless, surface roughness should be minimized, for it can limit components fatigue life and functioning. [17]

Another common defect in additive manufacturing is porosity, especially with aluminum alloys. Pores form from gas residuals trapped inside melted metal, generally caused by excessive energy input or process instability. [22] Furthermore, contaminants on the metal wire surface or shrinkage caused by incomplete solidification might cause porosity as well [23]. Porosity reduces significantly the density of the component, which leads to increasing probability of cracks. If the pores form on the surface, it increases the surface roughness and the difficulty of reaching desired dimensions. [22] Porosity can be lessened by ensuring cleanliness and quality of wire and substrate shielding gas and controlling the process parameters. Also, post-processing such as interpass rolling can be applied. [15] With material choice the probability of porosity can also be diminished.

2.2.2 Build up and path planning

WAAM is a flexible production method that can be used to form a wide variety of component structures. Often the structures are completely solid objects made by layers of several overlaid welding beads, which following a certain filling path, often in circular movement [24], [25]. Most common path pattern is unidirectional [21]. Deposition rate of WAAM is fast, there is a step effect between layers, and the heat input necessitates non dense path planning. Also, the points where the arc ignites or extinguishes are prone to defects and therefore, the path should be as continuous as possible with least number of ignite and arc-extinguish points possible. [18] Additionally, material can accumulate in curves or during change of direction and lack of fusion can occur in other weld bead side. These problems appear especially in the larger components. [26]

The cross-section of the single weld bead of WAAM has the geometry of parabola. Therefore when constructing multi-weld bead structures, the overlapping distance of different beads must be considered to keep the buildup stability [27]. Too small overlap results in lack of fusion and too large overlap to uneven layers and challenges for subsequent layers [26]. Figure 5 represents the cross-section of a bead layer. Optimal distance has been widely studied, and different models have been proposed. Ding *et al.* [28] developed a tangent overlapping model (TOM) based on geometry models of the overlapping beads. They determine the overlapping distance to be following $d = 0,738*w$, where w is the width of the single bead. However, Cao *et al.* defined $d = 0,637*w$ as the correct distance based on Gaussian and logistics and parabola functions [29]. Hu *et al.* remarked that the overlapping varies with different geometrical parameters, and to achieve stable overlapping process and flat top surface overlapping should in the range of (0,6317; 0,7732) [30]. However, Müller & Hensel pointed out [26] that although multiple theoretical investigations have been made to determine optimal distance between weld

beads, there is no sufficient universal tolerance range or stands taken on optimal process parameters or material behavior. They conducted an experimental study and discovered approximately 15-50% overlap to be optimal, depending on the process parameters. In conclusion, there are multiple studies that determine optimal overlapping distance for overlaid beads based on mathematical models. However, these models do not consider the influence of varying process parameters and, for example, different materials and thus may reflect reality poorly.

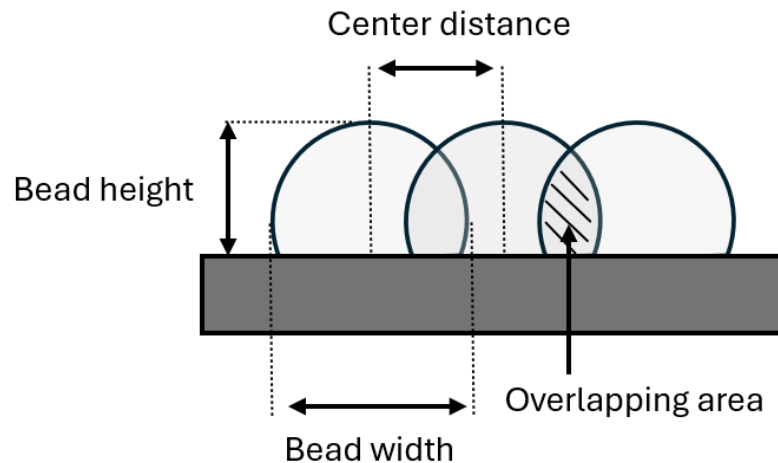


Figure 5. Cross-section of bead layer, adapted from [28].

WAAM is generally built up with contour wall which follows the outline of the component and following fill up. Developed methods for WAAM filling path strategies can be divided into three categories, continuous path, linear path and the combination of these two. The linear path includes the zigzag path and raster path. Raster path is simple and easy to implement, and it is best for large components for the lack of corners and curves. This fill path consists of parallel lines intersecting the contour. However, the lines edges are left discrete, and therefore the surface precision can be inaccurate. To reduce the surface inaccuracy, a zigzag filling path was created. Zigzag path has continuous wavelike movement, which means there is only one arc-ignite and arc-extinguish point per layer. This reduces and line points and improves efficiency. Zigzag filling path is the most used of all the WAAM filling paths.

The contour filling path is formed by following an offset of the contour, which makes is easy and simple to use. [18] Every path in each layer is closed, and thus every path has end and start point. To minimize the start and endpoints spiral contour filling pattern can be used. Spiral contour filling pattern follows the contour, but individual paths are connected creating a spiral shape. This is great path solution for smaller scale objects, but in larger components the layers might start to accumulate towards the middle and inflict

some challenges. [26] In the end, the most suitable filling path is determined based on the fabricated component. General classification and filling paths are illustrated in Figure 6.

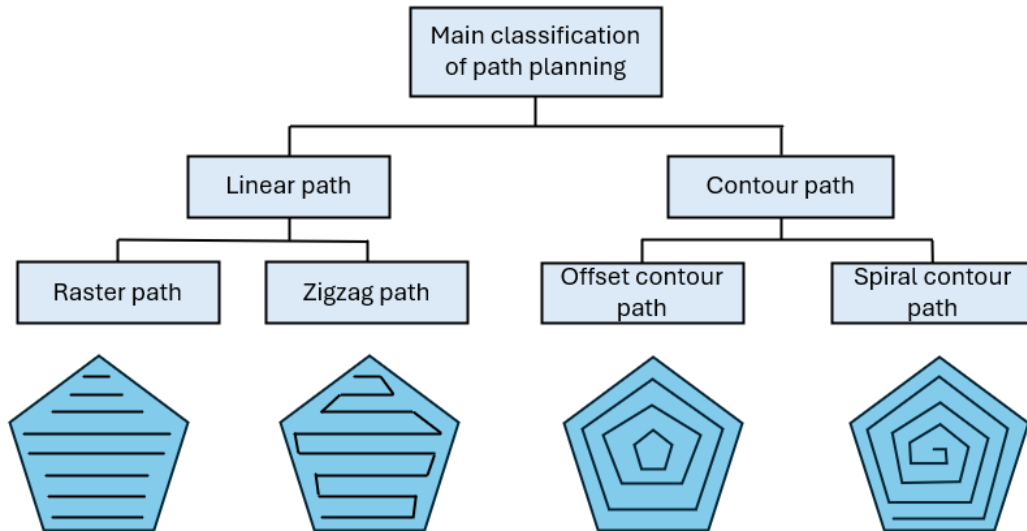


Figure 6. General filling paths, adapted from [26].

WAAM can also be used to build objects that require thin walls, that are topology optimized, or have self-supporting structures, made by single bead deposition [24], [31]. These thin walls can be built by single bead walls, or with two or more overlapping parallel beads and/or with weaving path. [21]

The weaving method is also called as “oscillating” or “swinging” and is furthermore elaborated in Figure 7. Despite being a relatively new method, it has already gained attention. Unlike traditional deposition process, which moves forward alongside the deposition direction, the weaving deposition process moves oscillating laterally whilst it is moving forward, creating a zig-zag path [32]. With weaving deposition, the covered area in each layer is larger causing faster build up, with the addition of more evenly heat distribution reducing thermal distortion. However, it exhibits poor surface quality. In addition, the programming is more challenging. Therefore, the choice between single bead and weaving strategies should be made with consideration of geometry, desired material properties, and conscious trade-off between build up time and surface finish. [33]

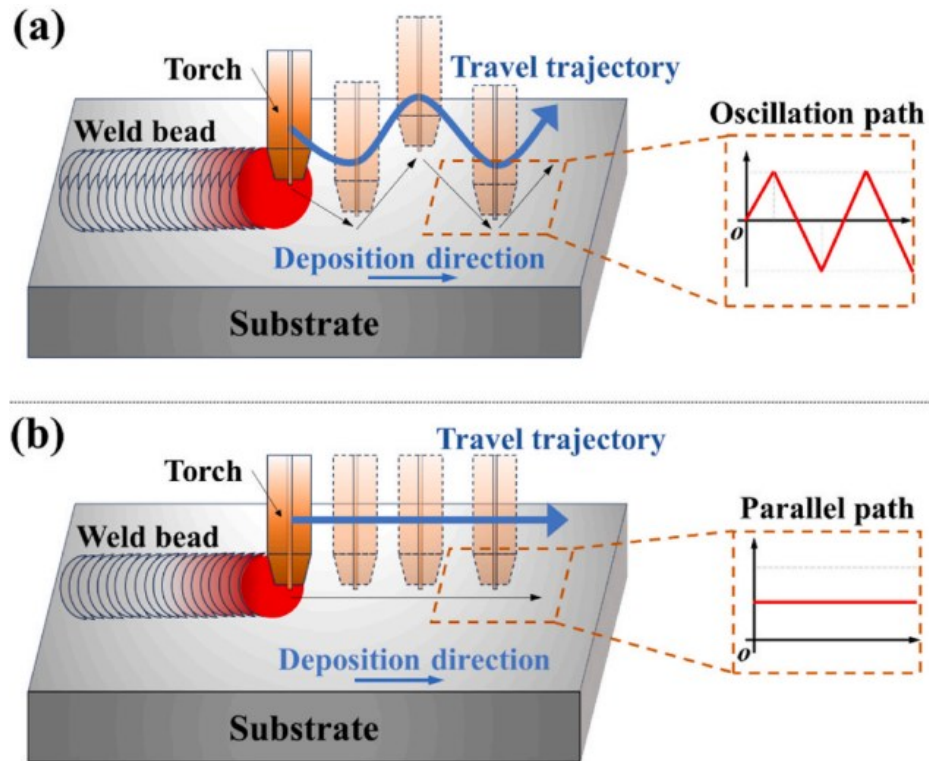


Figure 7. Parallel deposition path compared to weaving (oscillating) deposition path [32].

Industrial robots often utilize processes that use waving deposition path. Naturally, since the path is not simple and unidirectional, more process parameters are required to determine weaving path. The three main parameters to control the weaving movement of deposition are parallel travel speed, weave length and amplitude. [34]

2.2.3 Component geometry and characteristics

2,5D structures refer to complex three-dimensional (3D) substrates which can be fabricated by controlling and stacking 2-dimensional surfaces layer-by-layer [35]. In other words, 2,5D components are a three-dimensional construction in two-dimensional space. 2.5D components are known as lightweight designs with enhanced safety and are used in automobile and aerospace sectors due to their good energy absorption qualities. One efficient way of manufacturing these components is additive manufacturing. [16] For example, casings, housings and simple flanges can be classified as 2,5D geometry. Figure 8 illustrated different 2,5D profile geometries.



Figure 8. Nature inspired 2,5D geometry parts [16].

Housings, also known as casing, hub, tray etc. is a core component of an engine. They are widely used in generators and in electric motors and are mostly made from metals, such as steel, cast iron, stainless steel and aluminum alloys. Engine housings functions as a protective element, in addition to being a mounting frame for other components. Engine housings have high requirements for structural accuracy and performance. [36] Its quality affects significantly the fuel consumption, performance and service life of an engine [37]. Engine housings sizes and shapes vary based on engine types. Some structures contain two tray-like sides, and other housings are based on cylindric shape.

High geometrical accuracy requirements make engine housings challenging to manufacture [37]. Moreover, the demand to fulfill variety of requirements limits the utilizing of traditional technologies [38], as well as the desire to minimize the waste of a high-quality material. These disadvantages create a demand for alternative manufacturing technologies. Some studies have successfully manufactured different types of motor housings using additive manufacturing [38], [39]. These studies indicate that additive manufacturing can be used to produce engine housing successfully. However, these experiments were not conducted with WAAM, so further research is needed to draw final conclusions.

As it is stated before, there are not already made studies or designs for engine housing manufactured by WAAM. However, closely resembling geometries of tray-like housing can be found in two demonstrator parts. Firstly, Addison *et al.* [40] attempted to produce and assess a high complexity titanium (Ti_6Al_4V) part, which contained variety features that they had not been yet produced or were known to be problematic. These features included stepped wall, slot, wedge, tube and boss features, varying wall thickness, sharp corners, intersections, overhanging structures, round corner and raised level. The objective was to demonstrate that high complex parts with good material properties and high material integrity can be produced without expensive tooling or complex support structures using only readily available equipment. The final model was redesigned to support the manufacturing method. See the result below from Figure 9.

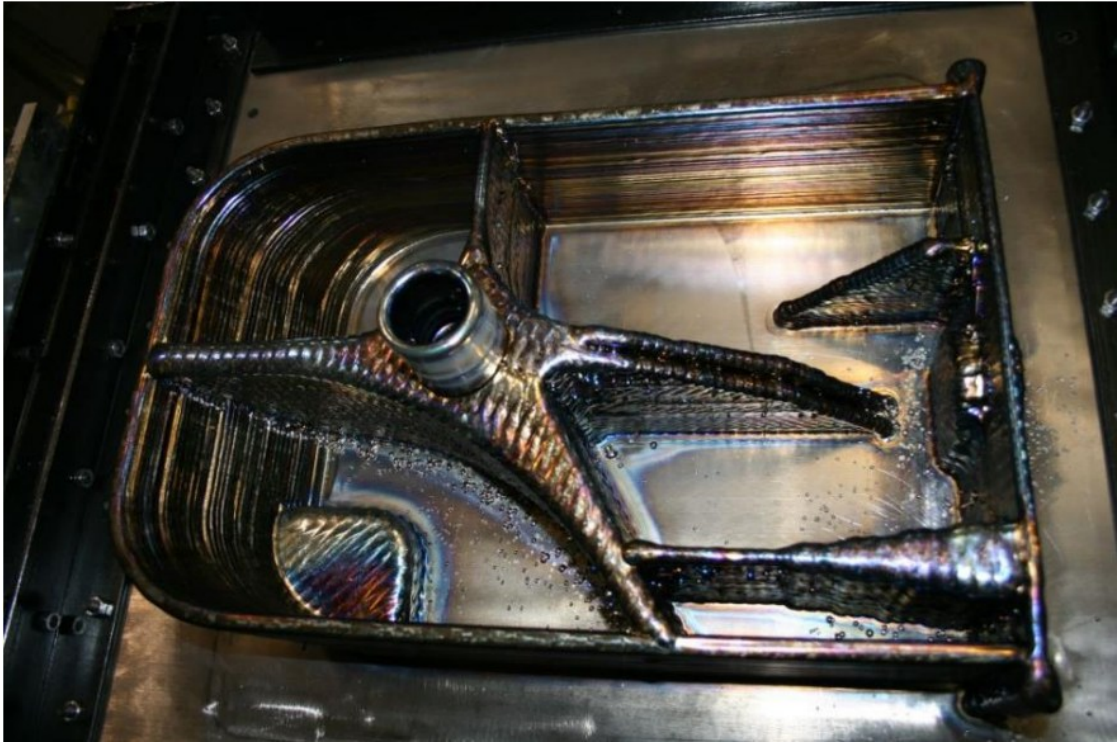


Figure 9. Demonstration part of WAAMs capability to produce different geometries and features [40].

The part was successfully built; however, they stated that a variety of lessons were learned during the process. Unfortunately, subsequent builds could not be made to continue this study.

The second demonstrator part was made by Suárez *et al.* [33] to explore WAAM capabilities and demonstrate its adaptability. The designed titanium (Ti_6Al_4V) part had relatively simple thin-walled structure, consisting of contour and intersecting wall structures with varying thicknesses. This study focused on different deposition strategies and path techniques and aimed to demonstrate WAAM's adaptability. Both single bead and oscillating deposition strategies were used. Special attention was paid to the junction points of intersections. Also with this demonstration, the final design was redesigned to support the manufacturing method. A flat titanium plate (Ti_6Al_4V) with dimensions of 20 x 260 x 170 mm was used as a substrate. See the resulted component below from Figure 10.



Figure 10. Demonstration part containing different deposition paths and multiple cross sections [33].

The printed part's dimensions were 260 x 170 x 45 mm. The single bead walls had width of 8 mm and oscillating walls had widths of 18 mm and 24 mm. A spatter could be seen in the oscillating walls due to directional disrupt in the delivery of protective gas caused by directional change. Post-Processing was deemed necessary to achieve final geometry of the component. Also, a heat treatment was suggested to enhance the mechanical properties. However, neither was carried out in this paper.

2.2.4 Traditional manufacturing of engine housing

Traditionally, engine housing is most often manufactured by precision casting or by machining. Both manufacturing methods have their advantages as well as a favorable operating requirement for the best usage. Nevertheless, several challenges are faced with these manufacturing methods when trying to fulfill multiple alternating requirements. [38], [41].

Casting is an important segment of the metal-working industry. Several different types of casting processes have been developed to produce parts for varying accuracy requirements and for different materials. However, all different processes are based on the same, simple idea. Liquid metal is poured into multi-part mold cavity and cooled down. Once the piece has cooled and solidified, it can be removed from mold. [42] To succeed in casting, attention must be paid to making high-quality molds with precise details. These molds can be either single-use or reusable if they have a protective coating to withhold the hot liquid metal attack or are not in direct contact with it. Casting parts can

be post-processed to achieve desired features and characteristics. Post-processing can be for example, heat treatment, machining, welding or straightening. [43]

Casting is essentially rapid pace of manufacturing with controlled accuracy, which makes it ideal for mass production [42]. Therefore, it is desirable manufacturing method for automotive casings, where volumes can reach millions. Furthermore, casting process can be highly mechanized and produce high quality parts with reproducible mechanical properties and surface finish. It can also reduce cost of machining, finishing and heat treatments. [43] Therefore, not surprisingly, most common manufacturing strategy for engine housing parts is casting Al-based alloys [38]. On the other hand, material selection, configurations and some physical considerations limit the usage of casting and might therefore lead to other manufacturing technologies [42]. Other drawbacks of this method include low quality caused by gas porosity, high surface roughness, relatively low geometric accuracy, need for post-processing such as machining and long wait times required by the process [38].

Some engine housings, an aero-engine housing for example, must function in extreme environments containing high temperatures, high pressure and high speeds. These housings are often made by machining. [41] Machine tool is considered one of the most important equipment in the industry, and systems such as five-axis machine tools have major role in manufacturing complex parts for aviation, aerospace and automobile industries. Just like other manufacturing technologies, machining continues to evolve. Higher efficiency and accuracy have been and remain as main development goals in the machining industry. [37]

Machining refers to an entity of subtractive process techniques. Generally, workpiece is shaped into final geometry by removing material progressively by cutting. Either the workpiece (turning) or cutting tool (milling) rotates with high speed, whereupon cut is caused by employing relative motion between cutting tool and workpiece. The stock of the workpiece can come either from another manufacturing process in a form of near-net-shape, or as basic a plate, rod, bar etc. In the former case only, necessary finishing is performed to achieve functional surfaces for the component. In the latter case often a large amount of material needs to be rough machined away, before finishing the part. [44]

Machining requires always a part program, which recount the tool paths and necessary process parameters. To form the program, the geometry, contours and material of final geometry must be known. Additionally, limitations of the machining process, geometry of the cutting tool and finishing characteristics must be considered. Without the modern

advent of computers, this can be a costly and time-consuming task. However, generally nowadays process looks as follows: a model of part is created with Computer aided Design (CAD) software, after which CAD model can be fed to the machining system with fitting production values, which completes a part program. Next the program is tested and then approved, following a release to the production. Part can then be mass produced with the same program with little difficulties, until part or process are modified. [45] Machining system objective is to create mass production of identical components with continuous quality without human interference [46].

Two of the most multi-purpose cutting machines are CNC lathe machine and CNC milling machine. They contain automatic tool replacer, that can change tools between different machining operations, without external measures and allow multiple machining operations to be performed in a one work setup. CNC milling machine can execute milling, drilling, reaming and tapping, whereas CNC lathe machine can perform grooving, boring, facing and other turning operations. [44] CNC machines main essence is computer-based controller, which commands programmatically servo motors that actuate machine axes. Nowadays CNC systems contain solid user interfaces, control auxiliary processes, can coordinate multiple paths and cell operation applications. CNC has developed from Numeric Control (NC) machines, which date back into 1950s. [45]

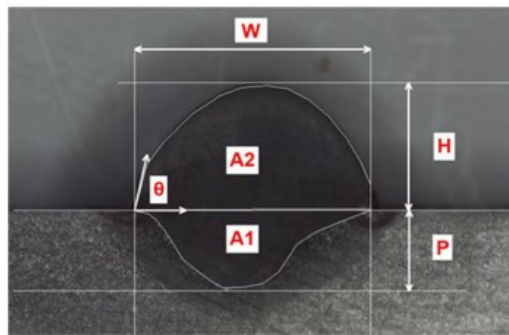
Machining is often utilized when production volumes are small and quality requirements high, or alternatively used material is challenging to cast. Furthermore, machining is a flexible manufacturing method, where small improvements and changes are easy to implement, even after the release to manufacturing. This is a clear advantage in the climate of modern technology. [47] Machined components often call for materials with high durability and with otherwise high-quality features (e.g. titanium alloys, nickel-based alloy) but alas poses challenges for its cutting processes. [41] Furthermore, machining can be energy and time intensive, have low buy-to-fly ratio and therefore generates a lot of waste, and can be costly compared to casting, for example [47].

2.3 WAAM manufacturing process

Primary stages in WAAM manufacturing are process planning, deposition and post-processing. One of the most important details in process planning is the consideration of deposition parameters. They should be carefully selected to achieve flawless components with good geometrical accuracy. Deposition stage can be incorporated with different sensors for real-time control and oversight of the process. Final post-process machining needs to be considered thoroughly to achieve adequate results. [48]

2.3.1 Process parameters

To acquire desired outcome from the WAAM process, process parameters should be carefully controlled. These process parameters are deposition width, wire diameter, layer thickness, wire-feed rate and welding speed [11]. Also, interlayer temperature and dwell time, torch and substrate angle, welding current, and contact tip-to-work distance should be considered. Each of these parameters have different effect on the part and functioning combination of the parameters must be found to achieve certain features such as low surface roughness and high mechanical strength [4] The functioning of the key parameters is elaborated below in Figure 11.



W: Width(mm)

H: Height (mm)

P: Penetration (mm)

A1: Penetration Area (mm²)

A2: Reinforcement Area (mm²)

Figure 11. WAAM process parameters [49].

Deposited layer geometry depends mostly on welding speed, wire-feed rate and heat input. These parameters interact so strongly that they cannot be treated as entirely separate variables. Furthermore, different combinations of these parameters might result in similar geometries. [50]

Heat input is a measure of supplied energy to the weld per unit length. It has a linear correlation with weld bead geometry. During build up, every layer acquires additional heat which causes heat accumulation. Wire-feed rate and welding speed are the main process parameters to control the heat input, and more specifically their ratio wire-feed rate/ welding speed. It should be noted that to change welding bead geometry significantly, these parameters must be changed so that the value of the ratio changes. For example, decreasing this ratio by increasing welding speed means that less heat is transferred to the material and less material is deposited per unit length. [49] These decreases both the width and height of the deposited layer. From these two, the difference in height is rather minor but difference in width is significant. Moreover, increasing welding speed decreases penetration and roughens contour of the layers. [50]

The number of passes required to build a part depends on wire-feed rate. When increasing wire-feed rate the width of the layer decreases but the height of the layer increases.

This is since more welding arc energy is needed to melt the higher wire-feed rate, and so the lack of fusion in the layers decreases the deposition width. Also, the weld penetration decreases which produces more convex clad layers. When increasing the heat input there is an increase in the deposition width and weld penetration. [50]

Deposited layer geometry determines the characteristics of deposited walls. In the example above, there is an increase in the wire-feed rate and heat input. This results in a relatively wider wall width and higher flatness deviation. Changing parameters such as increasing the welding speed affects the geometry of deposited layer and produces less flatness deviation and narrower bead. [51]

Creating the required metallurgical bond between layers requires re-melting thin section of previous layer, regulating the cooling rate and lessening residual stress. One crucial parameter in the multi-layer process is therefore the pre-heat or interlayer temperature. [52] Pre-heating the substrate is one way of balancing layer geometries through build up [4]. The interlayer temperature of the previous layer or pre-heat of the substrate also affects the geometry of the deposited layer. When the temperature is higher the deposition width increases and the height decreases. Furthermore, lower heat input can be used which can help increase the dimensional accuracy of the part and improve the uniformity of the deposited layers [52] So, regulating the inter-layer temperature properly leads to stable and smooth surface while deposition. Thus, another parameter comes crucial, the dwell time, which is essentially the cooling time between layers to obtain the desired interlayer temperature. Dwell time is often determined as a tradeoff between production time and desired production features. [4]

Heat input has an inversely effect on hardness values, as opposed to, cooling rate and local composition which have a linear effect, and they are all related to the final microstructure [49]. Furthermore, the heat input increase affects the cooling rates and the parts microstructure and therefore mechanical properties, for example with low interlayer temperature and low heat input and therefore short dwell time a hard and smooth walled component with lower stiffness can be printed [51].

With each deposition layer, the part experiences thermal stress due to heat input and it can raise residual stresses. Now, first few layers require more heat input to gain good wetting on the substrate. Heat input should be then gradually reduced during building process, if not the height dependent profuse accumulation of heat can affect the layer width and geometry in an unwanted way [50]. Nonetheless, with multilayer deposited parts three distinctive zones can be identified, lower, middle and upper zones. Lower zone is located near the substrate, which helps it cool down faster producing higher

hardness for this section. In the middle part accumulated heat reduces cooling effect making this section lower in hardness. The upper zone has the highest hardness, for it does not experience repeating re-heating. [51]

A variety of shielding gasses are used in WAAM process. The object of shielding gas is to produce a gas flow around the arc to protect the molten pool from atmospheric air's damaging effect during deposition. With different metals, different kind of gasses and gas blends are used. For example, popular use with austenitic stainless-steel is a mix of argon and carbon dioxide. [53] Selection of shielding gas should be just as important than selecting any other process parameter, for even though you only change the gas, bead shape, bead penetration and metal-transfer pattern can transform drastically. For example, different the amount of carbon dioxide in CO₂ + Ar shielding gas blend changes the heat impact in the deposition, which effects bead geometry. Correctly selected shielding gas enhances the stability of the process, improves build quality and can enhance the production efficiency. [54]

2.3.2 Process flow/steps

WAAM manufacturing process consists of particular stages, which are presented in the Figure 12. To start with WAAM process, a 3D model of final geometry must be created. The shape and size are often altered to facilitate the manufacturing process [55]. Therefore, often large holes are closed, machining allowance is added as well as fillet radii and lead in and out structures to the wall ends [40]. Reworked geometry can then be uploaded to the slicer program, to form a layered geometry. Oftentimes test walls are printed to investigate proper slice layer heights. Furthermore, test walls are used investigate and finalize proper process parameters. [55]

In the next step, the algorithms for the torch movements are considered. The algorithm is based on the part geometry, selected build up strategy and wanted end result. Thereafter, sliced geometry model can be loaded into software environment, in which the deposition head operates, aka to the robot arm or CNC system. Generally, loaded geometry model is in G-code format. The software environment may contain solutions for simulating or programming the robot arm/CNC system, in which the deposition program can be finalized. If robot arms are used, created deposition program may need to be translated into robot program. [55]

After completing and downloading the program to the deposition system, possible errors should be checked. If checking has been successful and the torch trajectory is deemed to be correct, the process parameters can be set. Thereafter, the deposition can be started. [55]

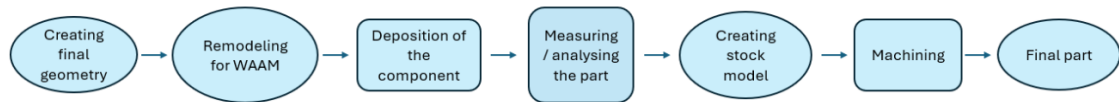


Figure 12. Flow chart of different production phases in WAAM manufacturing process.

One of WAAM advantages is the ability to manufacture components with one production machine in one step. During deposition, the kinematic system and welding source interact with each other to ensure a stable process. Some quality effecting abnormalities might still appear during build up. To detect them, various kinds of monitoring systems can be used. These sensor systems can be based on thermal, electrical, acoustic or optical measurement methods, and used sensor methods should be selected depending on the investigated quality characters. It is recommended to use more than one data source to create a reliable and stable monitoring system. [56] For example, IR camera can be used to measure interlayer temperatures of multilayer structures in order to achieve identical circumstances for every deposited layer [10].

After successful deposition component may be declared as finished if there is no intent to post-process. To verify the quality of the component and manufacturing process, an evaluation should be conducted. These can include precise measurements, 3D scans and model comparisons, for example. [10]

If post-processing is required, the next step is to create a machining path. To start, the deposited part's dimensions should be measured and obtained, so that the shape accurate geometry of deposited part can be used as a stock model. Thereafter, a cutting path can be created and verified by a simple simulation. These steps can be completed by using Computer Aided Manufacturing (CAM) program, for example. Before, machining the compatibility of WAAM process coordinate origin and machining coordinate origin must be confirmed. Finally, a post-processing machining can be performed. [10]

2.4 POST-PROCESS MACHINING

As mentioned above, WAAM manufacturing process can produce large components, but almost without exception part has poor surface quality and accuracy. Furthermore, warping or other distortions might appear. To solve this problem machining such as milling is used as a post-processing operation. According to Gillespie [7], combining WAAM and machining can produce better surface finish and closer tolerances, in addition to eliminating the useless or impeding support structures. Smoothing or polishing can even surface cracks, reduce stress risers and create more aesthetic appearance.

2.4.1 System setups and process strategies

Across the literature one can find multiple ways to combine AM and machining processes. All of which share a common objective, printed object is to be designed and produced as near-net shape object, so that minimum amount of material can be removed during machining. [20] Differences arise from the used equipment as well as from different process strategies.

One common option is to use multitask machining with one setup for both processes. Modern hybrid equipment consists of 3-, 4-, and 5-axes machining center with the additive process and implements two functions (WAAM and machining) on the same bed one after the other. This system has the advantage to achieve tighter tolerances. [7] Moreover, when manufacturing is completed in one setup cutting defects caused by misaligning the work origin can be eliminated. Unfortunately, cost of these hybrid manufacturing machines is quite high, which severely limits their usage. [20]

In the other system setup, there are separate and independent additive manufacturing processes and machining systems. For example, Hanamoto *et al.* created first the near-net shape of the final product with WAAM setup and then moved the component to machining system. Compared to hybrid machines, robot based systems are more economical to acquire. [20] For this and their flexibility, these types of setups are simple and most commonly used [7].

Machining can also be implemented as a part of additive manufacturing process cycle [20]. With this strategy, only one setup is required, and it can consist of two cooperative robot arms [9], or alternatively of multitask hybrid machine [7]. With two cooperative robot arms, one has a welding torch for WAAM system and the other has a milling tool as a machining system. After the desired number of layers are printed, the milling arm mills away the top and side surfaces of previous print layers to facilitate following print layers and to obtain good surface quality and desired geometric and accuracy. Printing and milling cycles are then repeated until the whole part is created. [9] Hybrid machine can similarly switch seamlessly from deposition tool to machining tool within additive manufacturing process cycle [7].

2.4.2 Considerations of design

Using hybrid manufacturing process affects the design of the produced part. The inclusion of the post-processing must be kept in mind as early as the designing state and for example, adequate machining allowance must be added to the geometry of the part. Moreover, removal of extra material leads to unnecessary material, time and cost waste, and so the minimum amount of material needed to be removed must be determined.

Fuchs *et al.* furthermore suggested that the amount of material that is to be removed should be larger than the occurring inaccuracies that occur in the deposited wall structures. They proposed that 125% of the maximum height point of the surface should be removed to ensure high surface quality. [57]

Some geometries may pose challenges for post-processing. Fuchs *et al.* discovered that start and end zones of wall structures might have to be removed to prevent critical tool contact. Naturally these zones need to be taken into consideration when designing machining strategy and therefore the part [58].

One of the challenges of post-processing is to align the coordinate origin of the deposition process and the machining accurately. It can be hard to determine origin coordinates from the irregular surface of the deposition if the process has multiple setups. One solution to match the origins of the WAAM and post-processing is to make a groove to the base plate as a pre-process. Then the base plate and deposition path can be aligned. [10] Other is to use small, fabricated objects (35 x 155 mm) on a substrate fixed on a reference section, and using a corner as a work origin [20].

Another discernability that produces challenges is the difficulty to predict accurately the silhouette of the workpiece. This complicates the creation of fitting machining paths. [10] Often advanced WAAM process requires a precise measurement method between these processes to define sometimes unpredictable end shape of deposited part [20].

2.4.3 Machining WAAM component

Machining a deposited part has some differences compared to machining a basic raw stock block. The final surface quality of the part is not only dependent on basic milling parameters such as spindle speed and tool-feed rate but also dependent of the WAAM parameters such as wire-feed rate and travel speed. This is since the cutting depth should be determined by the deposited bead geometry. This is particularly important if the machining is implemented inside the WAAM process cycle. [9] Another difference comes from the surface of the machined part. Deposited parts have wavy and geometrically low accurate surface, in which the surface hardness might vary. This unfortunately is not ideal machining surface and can cause instability in the machining process, such as chatter vibrations, which might lead to lower tool life, and rougher surface finish. [51]

Differences arise below the surface as well. AM parts have unique microstructure and therefore unique material properties, and this must be taken into consideration. [59] For example, Awiszus *et al.* found [60], that stainless steel (1.4403) WAAM parts have ori-

ented dendritic microstructure, which means that mechanical properties have low directional dependence. Furthermore, they acquire high cutting forces but have lower hardness (in comparison) due to local microstructure composition.

Some guidelines for machining a WAAM component can be found from the literature. Machining direction should be considered in relation to build-up direction [60], and feed direction should be the direction of the smaller waviness, to keep the average cutting force stable [58]. Moreover, using conventional calculations for cutting force is not recommended [60]. However, corresponding values or equations for machining a WAAM component have not yet been developed.

2.5 PROCESS AND COMPONENT EVALUATIONS

WAAM is often described as an effective, economically and ecologically friendly manufacturing method, and there lies its favorability over traditional manufacturing [61]. However, across literature the precedence of WAAM seems to alternate. In this section we take a closer look at literature of economic and ecologic analysis of WAAM to investigate, in which situations WAAM has been found to be a better choice compared to traditional manufacturing.

2.5.1 Economic analysis

One way of determining systematically the cost of an asset during its life cycle is Life Cycle Costing (LCC) method. It includes determining the significant cost elements, suitable cost model, and utilizing collected cost data. Cost elements can include machine cost (cost of tools, jigs, fixtures maintenance and tooling), material cost, cost of consumables (energy, shielding gas, cooling fluid etc.), post-processing cost and labor costs (operator, preparation time, set up time, supervision). [62], [63]

The above can be roughly interpreted as the following: the more material, consumables and labor is used, the more expensive manufacturing is. Therefore, things such as geometry, material and post-processing parameters affect the overall cost. Kokare et. al. found in their study, that for simple geometries such as wall, machining can be most economical solution, but if complexity of geometry increases or some other factor reduces the material efficiency, WAAM is less expensive alternative [62]. Another study made an interesting conclusion regarding post-processing and material allowances, for post-processing accounted for two-thirds of the WAAM production cost of marine propeller and WAAM was considered most economical approach when material allowance was under 4 mm [63]. Priarone *et al.* considered medium-to-large components produced with different materials and found that there are notable differences in favorability of WAAM,

manufacturing with aluminum had considerably lower-cost with WAAM, steel on the other hand with machining and titanium was in between [61]. Kokare *et al.* investigated the influence of batch size from 1 to 50 and found that for batch sized over three, WAAM is more cost-friendly, making machining better for single-unit production [64].

2.5.2 Sustainability analysis

Sustainability of a manufacturing method is most often measured with Life Cycle Assessment (LCA). LCA is a popular method for calculating ecological impact of process or product across its life cycle stages. This analysis takes into consideration environmental impacts of raw materials, energy usage, other resources, waste and emissions, and uses life cycle inventory data to form calculations and conclusions. This inventory data can be collected from experiments, literature sources and legitimate databases. [62] Across literature a cradle-to-life LCA is most often performed for WAAM.

Generally, cradle-to-life focuses on the timespan of the product from natural resource to the factory gate, including the impacts of harvesting of natural resources, formation of stock material, transportation, and finally the manufacture of the product. Production chains of WAAM and machining components are demonstrated in Figure 13. Now, if we compare machining and WAAM life cycles, we can see that the differences lie in the production and formation of stock material and part manufacturing processes. For WAAM there is the formation of wire feedstock which usually contains hot rolled steel billet that forms a rod, followed by wire drawing. The manufacture of the product requires the feed stock material, substrate material, shielding gas and energy (power consumption of electric arc) all of which can be measured during deposition. Post-processing machining requires additional power, which also can be measured. Lastly, comparing the weight of consumed stock wire and final product, an manufacturing material efficiency can be measured. [62], [65]

On the other hand, with CNC we can assume raw stock is formed by hot rolling a steel billet into bar, which then undergoes a rough milling. The manufacturing energy (of producing component) consumption depends on machine, machining method and material removal rate, efficiency and length. Other used resources are cutting fluid and compressed air. Again, manufacturing material efficiency can be measured by comparing weight of the raw stock block and the final product. [62]

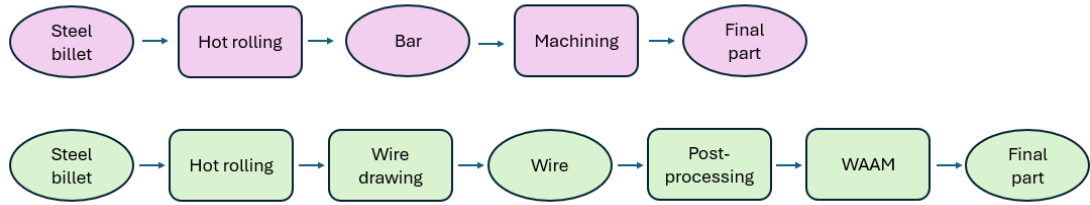


Figure 13. Production processes of WAAM and machining manufacturing technologies.

Different studies comparing LCA of machining and WAAM can be found from the literature [62], [63] [61], [64], [65]. The results of these studies vary, some found machining to be more sustainable and others WAAM. Therefore, following can be inferred: sustainability of product is affected by number of different aspects, such as material efficiency, geometry, material, size and so on. [62]

The complexity of geometry affects its material efficiency significantly. Increased complexity and wall curvature lead to lower material efficiency for CNC machining. This is caused by increase of removed material and therefore and increase in resource consumption, making CNC less sustainable. In comparison, material efficiency of WAAM is not affected much by the complexity of geometry. [62] Another study where object of interest was solid-to-cavity ratio (same as buy-to-fly) made similar conclusions, where change in foregoing ratio did not affect much the WAAM results, but had noteworthy effect on sustainability and cost of machining [65]. Priarone *et al.* conducted that remarkable reduction CO₂ emission, energy and resource demands can be seen in WAAM manufactured medium-to-large components, especially with aluminum and titanium materials [61]. Similar conclusions were made by Kokare *et al.* stating that WAAM is generally found to be more environmentally friendly compared to machining, and if component size is increased 5 times, WAAM environmental impact is half compared to machined component [64].

Across the studies above, raw material production has the biggest impact on sustainability, for both machining and WAAM. For machining, 80% of the impact can be from raw material production, and in second comes energy usage of manufacturing. Moreover, WAAM as high as 60% of environmental impact comes from raw material production, followed by usage of shielding gas and energy/resources used in post processing.

Nevertheless, most studies cannot be widely generalized as they are heavily linked to certain materials, geometry and process parameters, and therefore a change of characteristics can significantly change the results. Thus, to form general guidelines, more research is needed to truly understand the economics and ecology of the WAAM. [63]

2.5.3 Productivity analysis

Productivity is important value, and crucial in surviving today's competitive world. One way of improving productivity is to reduce manufacturing times. [66] Manufacturing time can be considered as a productivity metric, but is good to keep in mind that it is also closely linked in cost analysis [61].

For WAAM manufacturing time is often measured manually, and it includes set-up time, deposition time, interlayer cooling time and time for post-processing. Supposing fixed deposition rate, WAAM process time increases linearly in relation to increased amount of deposited material. [65] For machining, total cutting time can be measured manually from manufacturing process or alternatively from toolpath simulation of CAM. In both cases a timeframe for setting up and preparation must be considered. [63]

3. RESEARCH METHODS AND MATERIALS

3.1 Methodological approach overview

This section investigates the design, fabrication and post-processing of WAAM + machining through two case studies. Figure 14 illustrates the adopted methodology of the current study. This methodology approach integrates experimental investigation, from designed geometry to deposition, post-processing and finally to evaluation of produced part. Purpose of this study to ensure a thorough understanding and evaluation of hybrid WAAM process and its influence on component manufacturing.

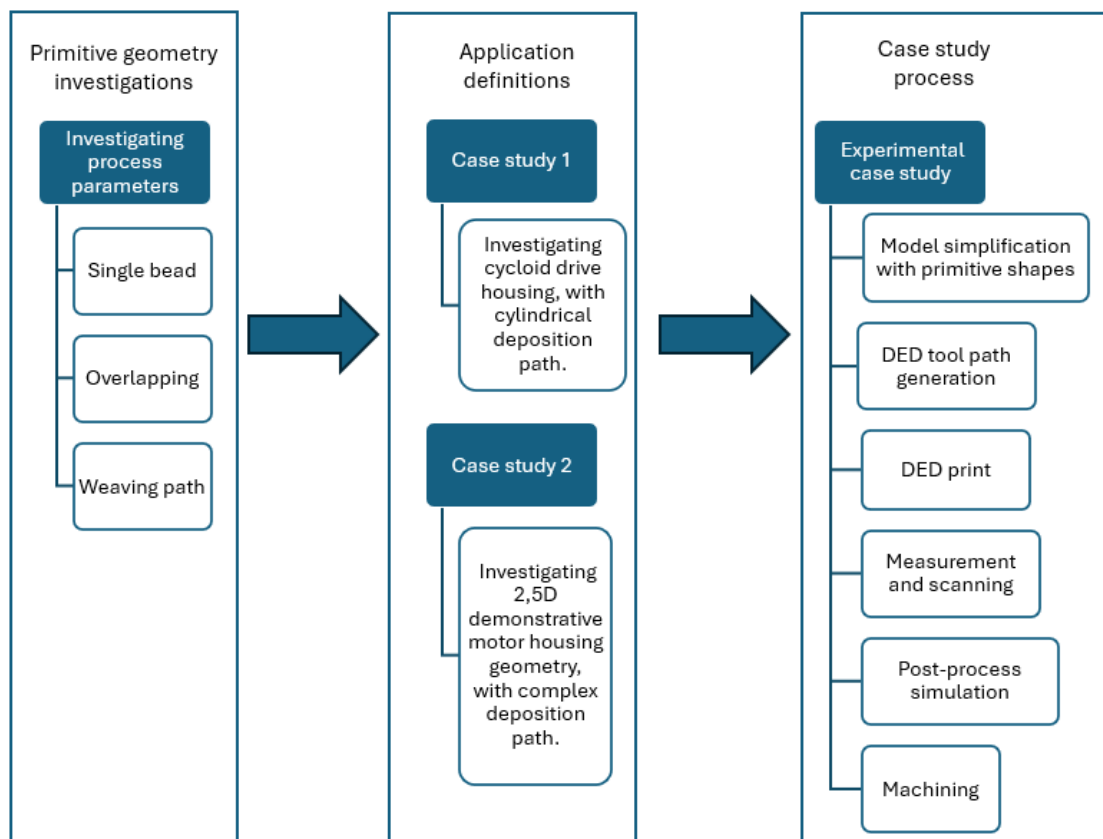


Figure 14. Chosen methodology approach.

This investigation consists of conventional process parameter investigation and two different case studies. The first case study 1 overviews simple geometry production with analytical evaluation including examinations on both physical component and the component in digital environment. Post-processing was studied through simulation and actual post-process machining. The second Case study contains more complex geometry, which enables investigation of the suitable build-up strategies and advisable utilization

of primitive geometries in path planning. Deposition is evaluated by fabricating and analysing a digital model, and machining post-processing is analysed with machining simulation in Siemens NX software.

3.2 Investigating process parameters

Several tests were conducted to find out suitable process parameters. Furthermore, the formation of simple geometries is investigated. Firstly, two single bead walls were fabricated to investigate suitable wire-feed rate and welding speed. After which several wall geometries were produced to define correct parameters for overlapping beads. The weaving deposition path was also studied with wall geometries. Based on these investigations, different primitive shapes with different deposition paths could be studied. These features included both cylindrical and block geometries.

The depositions were performed with ABB robot with a rotating table setup. Used power source was Fronius CMT and it was connected to the robot arm. The welding torch was mounted to the ABB robot arm. See setup from Figure 15.

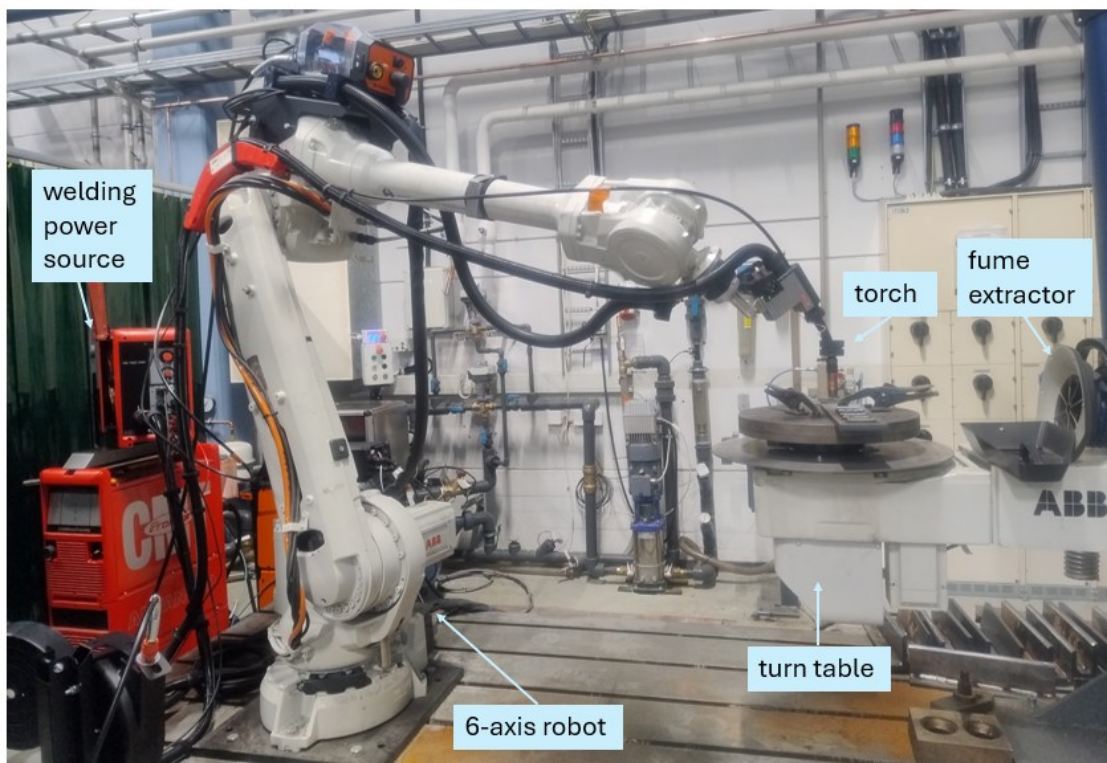


Figure 15. Demonstration of used setup at Tampere University.

Initially shielding gas UN 1956 containing 8 % CO₂ and 92 % Argon was used with the flowrate of 14,5 l/min. A steel S355 plates were used as a substrate. The substrate was brushed with steel brush to ensure cleanliness and the grip of the first layer. Used wire was TD-MAK10S with diameter of 1,20 mm. Interlayer temperature was maintained at

200 °C before each new layer deposition. Table 3 indicates the chemical composition of the G4Si1 welding wire.

Table 3. Composition of welding wire [67].

Material	C	Cr	Mn	Ni	P	S	Si	Total Cu
G4Si1	0,09	0,02	1,67	0,02	0,005	0,007	0,87	0,20

3.2.1 Single weld bead investigation

Two bead rows were printed to determine suitable process parameters, such as wire-feed rate and welding speed. The specimen's length was 100 mm, 10 layers were deposited on each wall. Layer height was set to 2 mm. The deposition was bidirectional to ensure proper structure during build up. Interlayer temperature was measured after each bead and subsequent layers were printed after the temperature reached 200 °C or under. See from Table 4 below the investigated process parameters.

Table 4. Investigating process parameters.

Specimen	Travel speed (mm/s)	Wire-feed rate (m/min)	Welding current (A)	Voltage U (V)
1	8	4	137	13.4
2	4	2	137	13.4

Produced specimen are presented in Figure 16. They had rough dimensions of 18 x 6 x 100 mm. As we can see, the specimen with higher welding speed and wire-feed rate has also rougher surface roughness. These specimens show clearly the trade-off between time and quality.

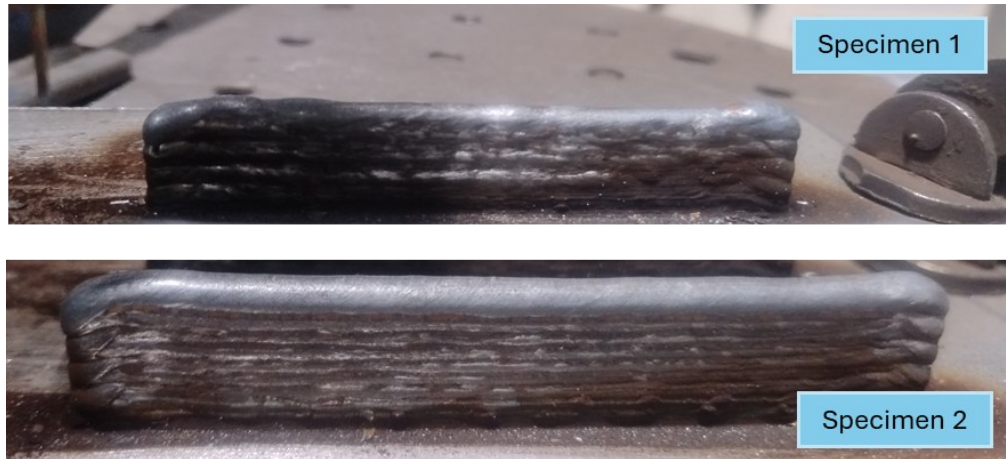


Figure 16. Produced wall specimens with different process parameters (trade-off between printing time and quality).

3.2.2 Overlapping parameter investigation

A series of overlapping parameter tests were conducted to determine adequate percentage for overlapping. Several papers in the literature indicated that the overlapping percentage should be somewhere between 63 – 77 %, based on mathematical models [28], [29], [30]. Furthermore, an opposing discovery was also discussed, based on series of experiments, the overlapping percentage should be somewhere between 15 - 50 % depending on process parameters [26]. It should be noted that overlapping can be calculated more than one way. In this study, we followed the model presented by Müller & Hensel [26], where the overlap is calculated as presented in equation (1) and used values are elaborated in Figure 17.

$$overlap (\%) = \left(1 - \frac{d(mm)}{w(mm)}\right) \times 100 \quad (1)$$

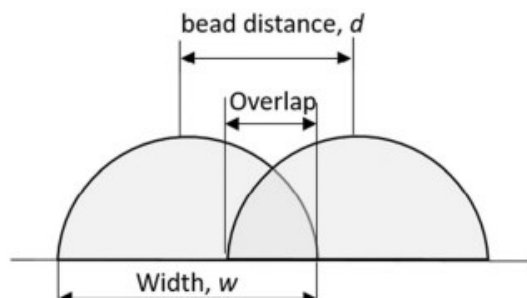


Figure 17. Cross-section of bead layer to clarify values in equation (1) [26].

Different shielding gases were tested as well. Initially shielding gas UN 1956 containing 8 % CO₂ and 92 % argon was used with the flowrate of 14,5 l/min. Wire-feed rate was 2 m/ min, welding speed 4 mm/s, and overlapping included three beads. Tested overlapping percentages were 25-50 %. Thereafter, a UN 1956 gas containing 2 % CO₂ and 98

% argon was tested. The overlapping percentages varied from 30-70%. Tests with both gases showed signs that fusing temperature for the metal was not high enough to produce proper melt pool, which resulted in several challenges. The overlapping percentage had to be extremely high (65-70 %) to bring all beads together, and this caused the layers to have inferior structure. Furthermore, with second gas (2 % CO₂ and 98 % argon) fully fused walls had low width of under 8 mm, and therefore the number of beads was increased to four. Second set of tests were conducted with the wire-feed rate was 4 m/min and welding speed 8 mm/s. Surprisingly, these printed walls did not differ much compared to first results. This might have resulted from the heat accumulation from adjacent bead rows. Even though wire-feed rate and welding speed were increased, remaining heat in adjacent bead rows could have produced enough warmth to fabricate similar melt pools resulting in similar bead geometries.

Another gas composition containing 18% CO₂ and 82 % argon was tested which was known to produce high fusing temperature for the melt pool. Since the last test indicated that two used process parameter sets resulted in similar walls, the faster parameters were used in all following investigations to achieve better efficiency. Studied overlapping percentages were 40%, 30% and 35% with 4, 4 and 3 overlapping beads, respectively. All these tests resulted in extremely promising results, most of all 35 %. Results from different gas investigations are illustrated in Figure 18. Except for gas exchange, the process parameters remain the same.

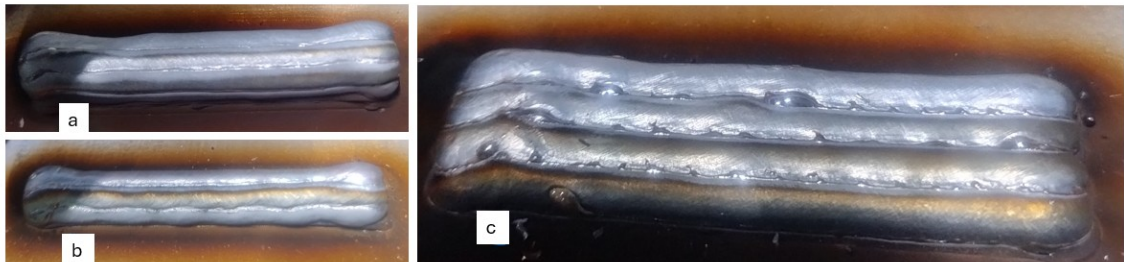


Figure 18. Three overlapping walls produced with (a) 8% CO₂ and 92 % Ar, 37,5% overlap, (b) 2% CO₂ and 98 % Ar, 40% overlap, (c) 18% CO₂ and 82 % Ar, 35% overlap.

Consequently, based on the results above, two 10-layer 100mm long walls were printed. The objective was to study the creation of full block-shape primitive with overlapping beads. Each multi-bead wall was printed with wire-feed rate of 4 mm/min and welding speed of 8 mm/s, and overlapping percentage was 35 %, latest shielding gas (18% CO₂ and 82 % Ar) was used. First multi-bead wall had three overlapping beads and produced a 14,5x22x100 mm block. Second multi-bead wall had only two overlapping beads and

it produced 11x20x100 mm block. Both tests were deemed as successful to define parameters for path planning of primitive blocks.

Next step was to investigate these parameters for a cylindric primitive shape geometry. Test continued with same parameters as before: wire-feed rate was 4 m/min, welding speed 8 mm/s, overlapping percentage was set 35%, shielding gas contained 18% CO₂ and 82 % Ar, used substrate was similar as to before and it was brushed before printing. Set diameter for the outer bead was 80 mm and inner circle diameter was calculated based on overlapping percentage. Layer height was set to be 2 mm. Ten layers were printed, and starting point of each layer changed counterclockwise $\frac{1}{4}$ of the perimeter between layers. Interlayer temperatures were maintained to be below 200 °C.

3.2.3 Weaving or oscillating

As an alternative deposition strategy, weaving was examined. Weaving strategy is alternative to the overlap deposition to reach wider deposition on deposition path. From different weaving shapes we used the zig-zag pattern where nozzle moves in X, Y- coordinate system and Z value remains as zero. The illustration of deposition path and main process parameters are shown in Figure 19.

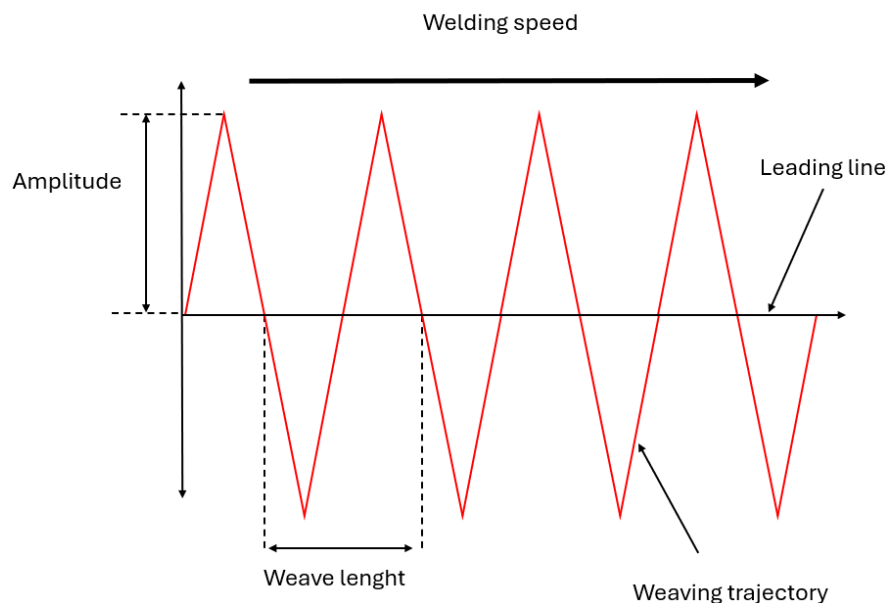


Figure 19. Weaving path and required main parameters, adapted from [34].

Different process parameters were tested, with varying welding travel speed, amplitude and wavelength. The goal was to produce wall of similar width than the final width of the wall in overlapping tests. Two different shielding gasses were also tested. Best results were obtained with following values: wire-feed rate 4 m/min, welding speed 2,5 mm/s, weave length 2 mm, amplitude 5 mm, shielding gas 8% CO₂ and 92 % Argon. Thereafter,

weaving was investigated with circular path, to produce an alternative for cylindrical primitive shape geometry. The aim was to produce similar dimensions as with overlapping cylinder. This resulted in 8-layer, circle with 76,1 mm diameter. Similarly to the overlapping deposition of circles above, starting point of each layer changed counterclockwise $\frac{1}{4}$ of the perimeter between layers and interlayer temperatures were controlled to stay under 200 °C. Figure 20 shows the results of two circular path deposited specimens for overlapping and weaving deposition strategies.

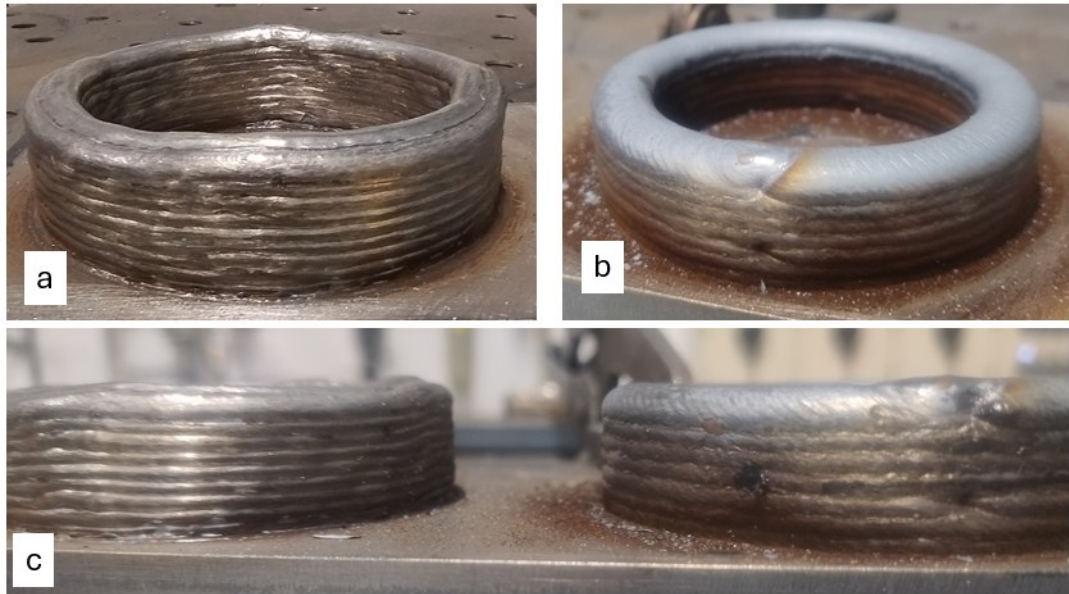


Figure 20. Results of circular path testing: (a) two bead overlapping deposition, (b) weaving deposition, (c) side profile comparison of overlapping (left) and weaving (right).

Both deposition strategies produced an object with solid structure. However, with weaving, the points where arc ignites and extinguishes had greater impact in the structure of the wall, and presumably there can be defects path planning, and hence weakening the structure of the component.

3.3 Creating case study geometries

During the design phase, the entire manufacturing chain was acknowledged. Furthermore, we capitalized WAAM's possibility of utilizing substrate, and freedoms in path planning. Challenges such as rough surface, misalignment from multiple set-ups, residual stress and distortion were considered. We followed general guidelines for WAAM components design proposed by Lockett *et al.* [5]. Final geometries were first created, and thereafter, they were redesigned to fit the WAAM + machining manufacturing method.

During redesign phase, the primitive shape geometries were utilized. Furthermore, different guidelines regarding using continuous path, tool accessibility, level on complexity, corner radii as well as part and feature dimensions were followed [5]. Machining allowance for post-processing was added based on values found in literature. In theory section we discussed Fuchs *et al.* estimation that machining allowance should be 125% of the maximum height of the surface [57]. Lockett *et al.* gave more general guideline of 1 mm for the surface roughness [5]. Additionally, features were designed to help with alignment of deposition and post-processing setups. Since we are using a robot arm set up combined with five axis CNC machine in case 1 a reference point was needed in the geometry of the part.

3.3.1 Case study one geometry

The focus of case study 1 is to investigate an alternative manufacturing method to produce cycloid drive housing. These components are commonly produced with machining, and this traditional manufacturing method is compared to hybrid WAAM + machining manufacturing. Therefore, the design model was redesigned to fit used manufacturing methods. This entailed defeaturing and simplifying the geometry, considering utilization of substrate, and adding machining allowance. The model was redesigned with Siemens NX CAD software.

Figure 21 illustrates cycloid drive housing part flow from assembly to reworked, de-featured geometry.

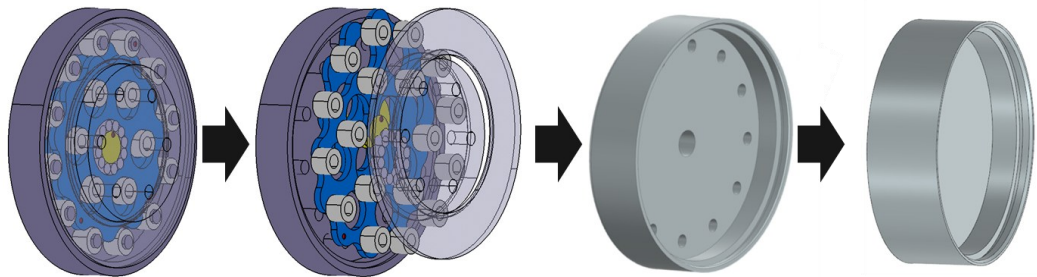


Figure 21. Geometry of case 1: Cycloid drive housing.

Initially, we assessed, if the final geometry is reasonable to produce with DED. According to Lockett *et al.* [5], there are four primary assessment criteria. First, the component should have a mass larger than 0,5 kg. The second and third criterion are connected to a bounding box's dimensions. Bounding box is a minimum cuboid (or cylinder in our case) in which the part can be enclosed. WAAM is a viable manufacturing method if bounding box has one or more dimensions over 20 mm, and all dimensions 10 m or

under. Maximum dimension is limited by the size of manufacturing cell. The last assessment criteria is the estimated buy-to-fly ratio which should be over 4.

Designed geometry met the criteria above. By assigning simple steel from NX material library, the mass of 0,78 kg is estimated. All the dimensions of the bounding box were between 20 mm and 10 m. After which we calculated the buy-to-fly ratio dividing the mass of the raw stock by the material of the final part accordingly: $1,59 \text{ kg} / 0,78 \text{ kg} = 2,04$. According to Lockett *et al.*, low buy-to-fly ratio might indicate that this component could be more cost effective to manufacture by machining. Although, it is good to keep in mind that buy-to-fly ratio varies between materials and therefore the estimate can be inaccurate depending on the material. [5] The first step of redesign was to consider the utilization of substrate. Embedded substrate seemed to be the best option since most of the material in the component is in the bottom plate of the part. Furthermore, by embedding it to the substrate we could have substantial material savings both in deposition phase and in post-processing. The second step was to simplify the geometry; therefore holes, chamfers, thread and groove were extracted. The remaining geometry was integrated with suitable primitive shape, resulting in cylindrical wall geometry. For aligning the coordinates, a small pin 4 x 5 mm was considered in the middle of deposition surface. This feature can be maintained when facing the raw stock material. Alternatively, a fixture can be used to ensure the centeredness of the component in a repeatable manner.

The wall of the final geometry was 4 mm at its widest point. From primitive shape investigations, we could observe that single bead walls had a width of 6 mm, and two overlapping beads had a width of 11 mm. These widths would result in 1 mm and 3,5 mm machine allowances per surface, respectively. However, it should be noted that uneven wall geometries have only been measured with vernier caliper and therefore the result is only a rough estimate. Therefore, most likely machining allowance per surface would be under 1 mm. To ensure sufficient machining allowance, a deposition path with two overlapping beads was preferred.

Dimensions for primitive shape geometry were defined accordingly. The outer radius of final geometry was 48 mm, and inner radius 44 mm. Machine allowance was distributed to both sides of the wall, 2 mm to outside and 5 mm to the inside radius. More material was added to the inner surface to ensure functional interface surfaces. Next, the deposition paths were defined. Since outer radius of deposition was 50 mm and knowing that one single bead to be 6 mm width, the outer circle path should have radius of 47 mm. Inner circle path was calculated with 35% overlap percentage and had radius of 42 mm.

The substrate had to be post-processed with deposition to avoid misalignment defects. To minimize material waste, the diameter of the substrate should be as close to final geometry as possible. Nonetheless, too large overhangs or projection in deposition layers could have led to dropping/pouring the melted metal. Thus, to ensure structural integrity substrate diameter was set to be same as the supposed outer wall of the deposition. For the height of the substrate there were fewer guidelines. Maximum feature distance was 14 mm, and adding 1 mm of machine allowance per surface, would result in minimum of 16 mm substrate height. However, Gupta *et al.* remark that with increased substrate size, the exhibited deformation decreases. They add that with thicker substrate plate, the internal ability to resist thermal residual stresses increases, which decreases the deformation. Therefore, by increasing the substrate size we can create a more stable base and improve geometrical accuracy. [68] Nevertheless, added material increases post-processing material waste, resulting in reduced efficiency and lesser sustainability. To determine acceptable tradeoff between geometrical accuracy and material waste, variety of different height substrates were examined. First substrate had 100 mm diameter and 14 mm of height, second 100 mm diameter and 40 mm of height. Last had a substrate with 96 mm diameter and 14 mm of height.

3.3.2 Case study 2 geometry

The objective for case study 2 was to investigate a more complex 2,5D geometry. A demonstrative geometry was designed following design features from existing WAAM component studies [33], [40], and typical features of engine housings. Basic design rules for WAAM disclosed by Lockett *et al.* [5] were followed. The model was designed using Siemens NX CAD software. Figure 22 illustrate the designed geometry.

The model contained a thin contour wall with round corners, supporting wedge features, intersections, raised platform and two different size cylinder objects. Addison *et al.* described similar features as challenging for additive manufacturing, nonetheless their team was successful with their deposition [40]. Furthermore, case study 2 geometry contains demonstrative fastening hole features alongside the center cylinder and rib features.

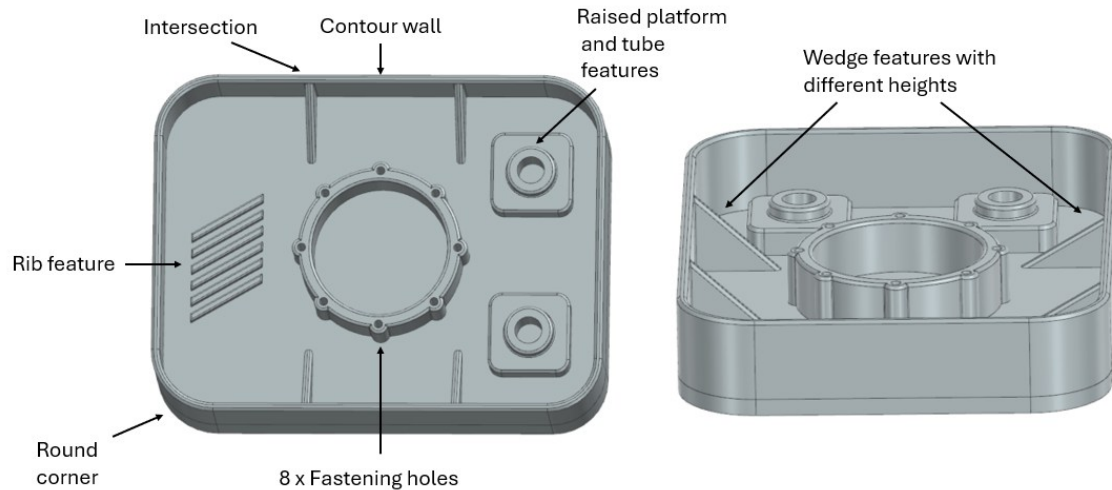


Figure 22. Case 2 final designed geometry.

Similarly to the first case study, four primary assessment criteria of *Lockett et al.* [5] were used here to evaluate produced geometry. By assigning material to the 3D model, we got an estimation of 1,36 kg for the mass of the component. Therefore, the first criteria (mass > 0,5 kg) were met. The second and third criteria were connected to bounding box dimensions. From Siemens NX we got the following bounding box dimensions 126 mm x 166 mm x 29 mm. Since all dimensions were over 20 mm and under 10 m, the second and third criteria were met. The last criteria stated that the estimated buy-to-fly ratio should have been over 4. By calculating case 2 buy-to-fly ratio, we got the following value: $6,65 \text{ kg} / 1,36 \text{ kg} = 3,4$. Fourth criteria was not therefore met, indicating that this geometry could be more effective to manufacture by other methods. However, buy-to-fly value of case study 2 geometry was only slightly below criteria value, and for example, with different material could reach this limit value.

Next the geometry was adjusted for WAAM + machining manufacturing method. First, we determined the utilization of substrate and build-up direction. Since we worked with a demo component and had a strong desire to minimize manufacturing time and used material we decided upon embedded substrate. When determining embedded wall, both advisable build-up direction for the features and efficient use of material was considered. The bottom of the geometry was the largest continuous area, and furthermore perpendicular to 2,5D geometry planes. Utilizing it as a substrate led to material and time savings and allowed deposition of every feature without any support structures.

The design was reworked to fit the manufacturing method. The structure of case study 2 geometry was quite simple 2,5D geometry, and therefore fairly accurate near-net-shape

deposition might have been possible to fabricate. However, further rework and programming for the deposition path would have been challenging and time consuming. Complex geometric features could have caused accumulation of material in turn points and create unpredictable geometries. Furthermore, WAAM's low geometric accuracy and poor surface finish could not have produced functional surfaces and would have required post-processing to form desired components. Therefore, we leaned on the strengths of WAAM as manufacturing method, high material utilization and deposition rate, and simplification of production process. Instead of trying to form complex feature structures, simple primitive geometries (such as cylinders and cubes) were used as the intricate features. The objective in determining primitive geometries was to simplify the rework and programming, reduce time needed in design and preparations and to form a solid base for post-processing. Primitive geometries were intended to be as near-net-shape possible to save time and reduce the use of extra material.

Thus, geometry was simplified, machining allowances added, and primitive geometries were used to prepare geometry for deposition. Small holes and chamfers were extracted. Machining allowance of 1,5 mm per surface was added to single bead wall structures. Rib structure was combined to form a solid platform. Centre cylinder was replaced with primitive shape cylinder. The platform combined with tube feature was reworked to a cubic shape. See redesigned geometry from Figure 23.

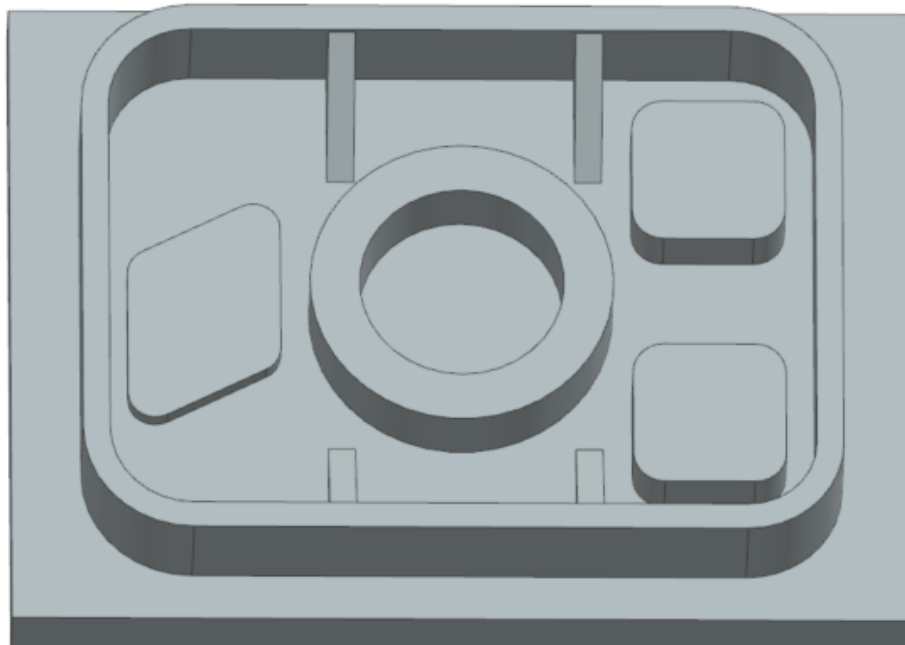


Figure 23. Case 2 redesigned geometry.

Designed bottom area had 5 mm height. Substrate with this little material is at risk of significant distortions, and furthermore the deposition time would be prolonged due to

longer interlayer cooling times. Therefore, we desired to enlarge the substrate plate, but kept in mind that added material increases post-processing machining, material waste and environmental load. Thus, a minimal amount of material was added to reduce the above-mentioned disadvantages but enough to ensure structural quality. The size of the substrate was increased in length, height and width directions.

After completing the redesign of geometry, the preparation for deposition could begin. The model was worked in UltiMaker Cura software. First the model was sliced parallel to the substrate plate, with 2 mm distance between the plates. 2 mm layer height estimation was based on overlapping cylindrical primitive shape investigation results.

Once the deposition strategy was considered, printing process was divided into two parts. The first part included contour wall, wedge feature, and platforms. The second build up consisted of cylindrical feature in the center. This build up strategy had the following advantages: by distributing each layer evenly to wide area, distortion in the substrate could be minimized. Furthermore, broad deposition area during each layer reduced the time needed in interlayer cooling. Cylindrical feature was deposited separately since it was fabricated with different deposition methods. Thus, for example, the layer height differed from the overlapping layer height. Furthermore, by fabricating the cylinder last, robot arm had more room to depositing material for other features and the risk of collision during build up was reduced.

The contour wall was fabricated with single bead parameters, as well as the intersecting wedge features. Rib feature platform was deposited with raster fill path strategy, and with 35 % overlapping beads. After filling path, the feature structure was bordered with a contour round. This aided in keeping the structure steady. Raised platforms with tube features were similarly deposited with a raster filling path strategy with 35 % overlapping beads and contour run. The orientation of filling path alternated in every layer. The starting point of contour wall was set at random on each round. Figure 24 illustrated the planned paths of first build up, these figures were taken in UltiMaker Cura software. White squares illustrate the arc-on points of each layer. Each layer's construction starts with rib feature platform, then other two platforms followed by the built of three wedge features. This is followed by deposition of contour wall and the last wedge feature.

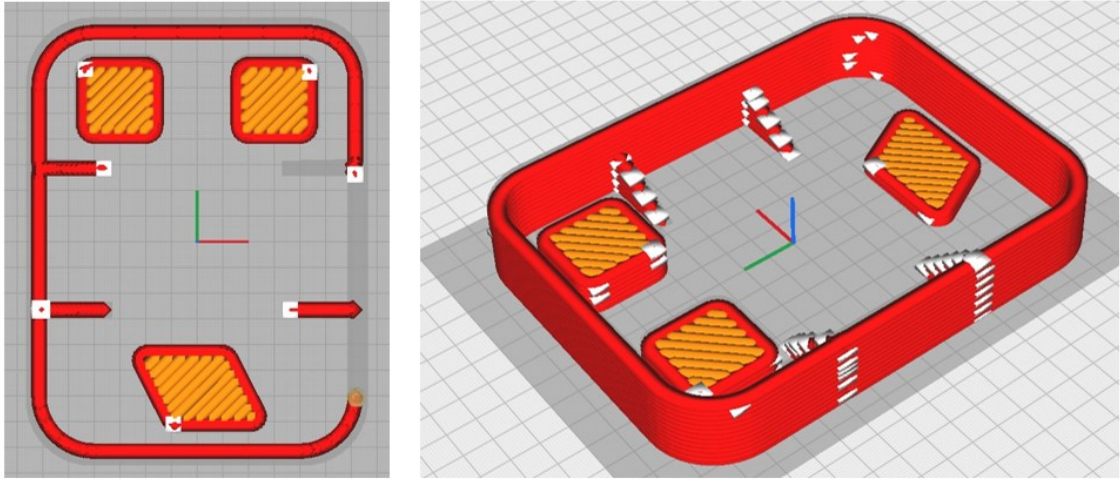


Figure 24. Planned path for first build up (left) and for the whole first build-up.

The cylindric feature was fabricated with weaving deposition strategy. Since the deposition method changed from overlapping to weaving deposition method, the slicing plane distance was changed to 2,5 based on previous weaving deposition investigations. The weave path was circle with 26 mm radius.

4. RESULTS AND THEIR REVIEW

4.1 Manufacturing case study 1

WAAM + machining manufacturing method was investigated by manufacturing case study 1 geometry. Multiple example parts were fabricated and analysed. Typical challenges for WAAM manufacturing, such as rough and wavy surface, geometric imperfections and distortions were studied by performing form fault measurements and examining scanned geometry. Furthermore, two physical components were post-processed by machining. Finally, manufacturing method was evaluated based on success of part production, and by comparison to existing literature.

4.1.1 Deposition of case study 1

Three components were produced, two with exact designed geometry (see 3.3.1) with outer diameter of 100mm, and one smaller component with outer diameter of 96 mm. All components had different substrate dimension. Parts were deposited one-by-one with same printing procedure and same process parameters.

First deposited part had a 100 mm diameter cylinder as substrate. It underwent face milling to even the deposition surface, after milling the height of the substrate was 14 mm. Furthermore, a small pin 4x5 mm was left in the middle to assist in the alignment of the coordinates. Previously best qualified process parameters were used: wire-feed rate was 4 m/min, welding speed 8 mm/s, shielding gas contained 18% CO₂ and 82 % Ar. 10 layers were deposited, and starting point of each layer changed counterclockwise $\frac{1}{4}$ of the perimeter between layers. Five second delay was set between outer and inner layer depositions. Interlayer temperatures were controlled be below 200 °C between each layer, and forced-convection cooling was enhanced with a small fan.

Before deposition, robot arm was calibrated by tracing the elevated pin and outer wall of the substrate with a calibration spike. Produced circular wall had with width of 10,5-11 mm and height of 17-18 mm, depending on the measurement point due to as-built surface waviness. Figure 25 displays the calibration with calibration spike and result of deposition.

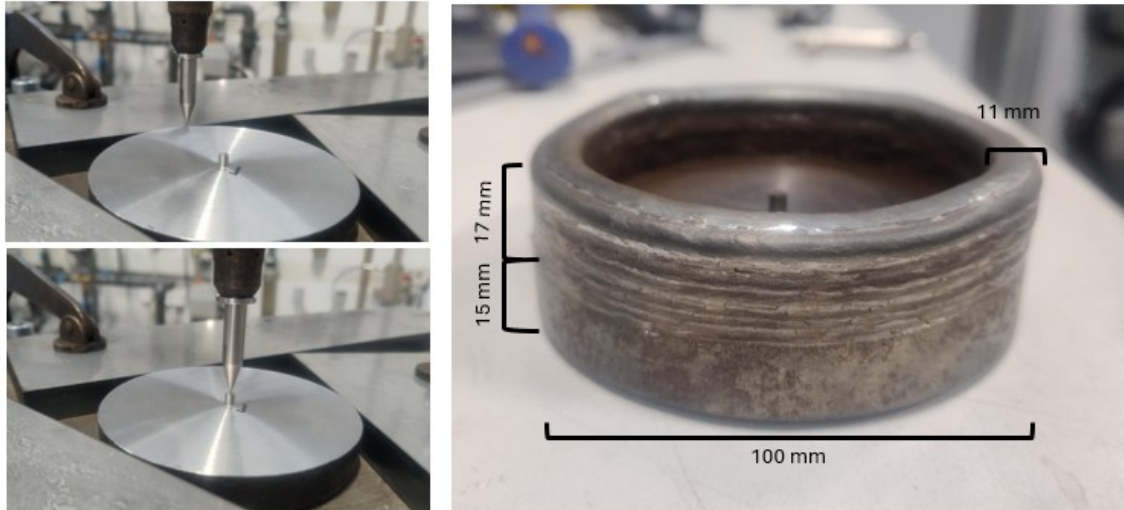


Figure 25. Calibration and result of deposited component.

Following values were measured during manufacturing, and substrate was weighted before and after deposition, to determine the mass of used material. The use of time was measured, both times spent to the entire process step (including idle, moving, deposition and cooling times) and the deposition time also known as arc-on time. Average shielding gas usage was measured as well as used current and voltage, from which used energy was calculated. See values from the Table 5.

Table 5. WAAM deposition values for case study 1.

Substrate mass (g)	Mass after deposition (g)	Shielding gas consumed (liter)	Set up time (min)	Entire deposition time (min)	Arc on - time (min)	Consumed energy (kJ)
860,7	1233,9	182,25	15	65	12,15	1521,79

Two additional equivalent geometries were produced with same process parameters. Fabricated components were named accordingly P1 had 100 mm diameter substrate with 40 mm height, P2 had 100 mm substrate with 14 mm height and P3 had smallest substrate with 96 mm diameter.

4.1.2 Form fault measurement

As mentioned in the theory section, WAAM as manufacturing process is prone to geometric distortions due to high heat impact. Geometrical form faults of two planar surfaces were studied comparing three deposited parts and one machined substrate. Studied surfaces and four measured components can be seen in Figure 26. From four examined

parts, three were deposited components with 10 deposition layers and one had undergone a face milling. Additional fourth component P4 demonstrated machined substrate before deposition, therefore it was only machined to use as a baseline for form fault values.

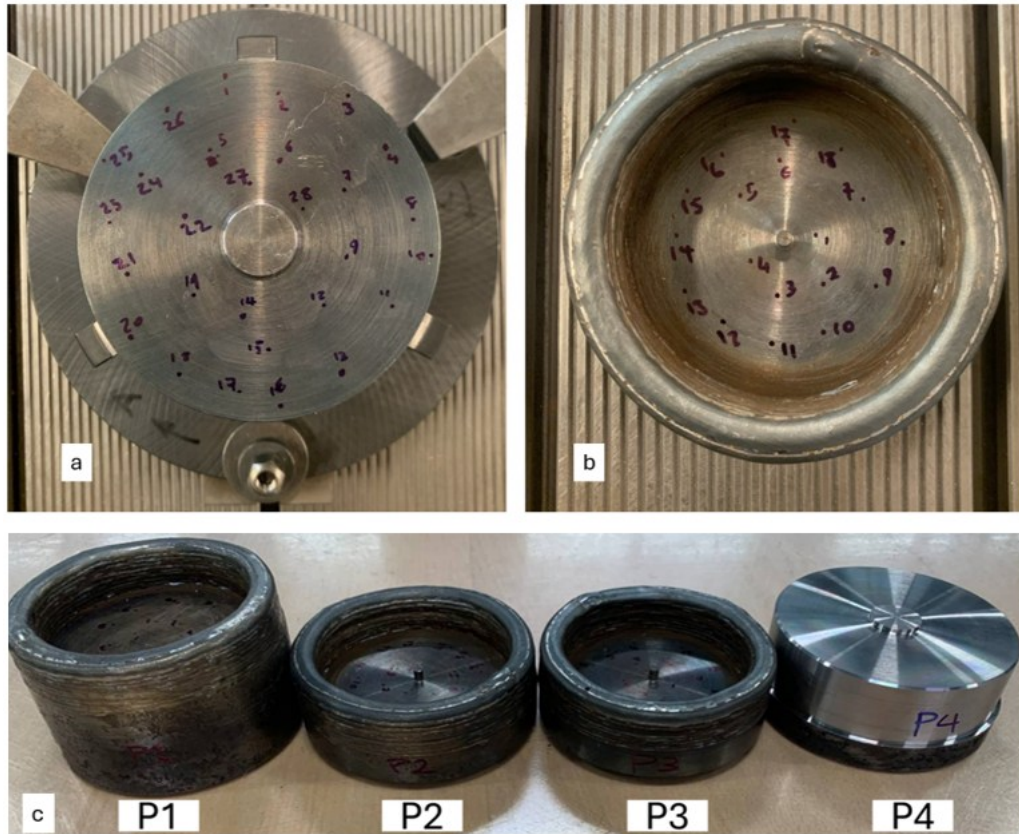


Figure 26. Defined measurement points, (a) 28 points for plane 1 and (b) 18 points for plane 2 and (c) measured components.

To define the measurement planes, a total of 28 points were randomly determined to surface 1 and 18 randomly selected points were determined to surface 2. Smaller amount of measurement points might have sufficed on this small and symmetrically deposited surface, however more points were defined to ensure avoiding any possible measurement errors. Roughly same point locations were used in all four parts measurements, and they were defined manually to avoid measurement errors caused by deposition spatters.

Parts were secured into a 3-jaw chuck, which allowed both a repeatable positioning as well as ample working space for measuring probe. When plane 1 was measured, the 3-jaw chuck held the inner cylinder of the deposited cylinder and plane 2 was measured with 3-jaw chuck holding the outside of the cylinder. A SIP coordinate measurement machine was used to measure the points. Table 6 below displays the outcome of form fault measures for plane 1 and plane 2 for all four parts.

Table 6. Results of form fault measurements.

Component ID	Diameter of raw stock (mm)	Height of raw stock (mm)	Form fault of Plane 1	Form fault of Plane 2
P1	100	40	0,033	0,023
P2	100	14	0,238	0,084
P3	96	14	0,251	0,104
P4	96	40	0,031	0,013

Across the table, form fault (distortion of the flat surface) for plane 1 is systematically larger compared to form fault in plane 2. Since Plane 1 is in direct contact with the heat impact of the deposition the effects are more significant which results in larger distortion. Furthermore, these results show initial form fault for machined face to be 0,031 for plane 1 and 0,014 for plane 2. Comparing the form fault of different deposited indicates that larger stock led to lower form fault errors and therefore to lesser distortions. Smallest raw stock cylinder led to over 700 % increase in form fault for plane 1 and over 450 % increase in plane 2, compared to largest stock cylinder.

Thus, one can deduct that to ensure minimum amount of distortion, increasing raw stock size should be considered. This is in line with remarks made by Gupta *et al.* [68]. This, however, clearly contradicts the geometrical and sustainability requirement for decreasing the size of the substrate to minimize post-processing machining. Therefore, additional optimization for substrate size needs to be carried out, to find acceptable trade-off between increased distortion and minimizing post-process machining and material waste.

4.1.3 Component scan and machining simulation

A 3D scan of deposited P1 was conducted with Hexagon AS1 Laser Scanner, attached to a Roamer Absolute Arm. Scanned model was first worked in PolyWorks Inspector and later in Siemens NX CAD software to produce a solid CAD art from point cloud. Figure 29 represents the scanned component.

Assessing the geometry from deposited part can be challenging. For example, measuring wall thickness from deposited part is difficult due to uneven surface. Measurements

with vernier calliper may vary by over one millimetre. From scanned 3D model, it is possible to examine the deposited geometry more clearly. Different print layers, starting and finishing points and high surface roughness can be observed. Furthermore, we were able to analyse wall thickness accurately. The results are illustrated in Figure 27. The red colour highlights the sections of the components with wall thickness below the specified value. Analysed wall thicknesses were 10 mm, 9,5 and 9 mm and 8,5. Machine allowances per surface of these sections result in 3 mm, 2,75 mm, 2,5 mm and 1,75 mm. The coordination alignment pin in the middle is excluded from review.

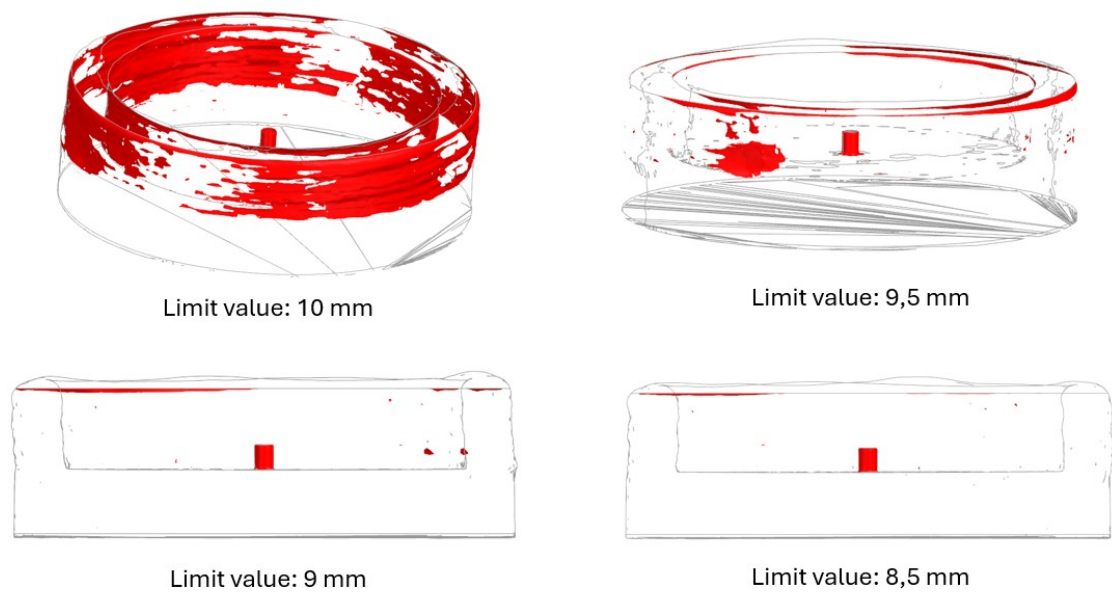


Figure 27. Wall thickness assessment, in which red colour indicates the areas below limit value.

Most of the wall thickness are in the range of 9,5 mm to 10 mm. With 9,5 mm limit value, we can observe a dimple in the structure of the wall. Concluding from dimples size, this is a systematic form error of several layers. This might be caused by robotic arm swing or wire deflection. Nonetheless, few small areas are below 9 mm limit value and merely little specks go below 8,5 mm.

Deposited part could also be observed as raw stock model, as illustrated in Figure 28. Final model was displayed as red, and transparency of grey scanned model was increased. Greenish colour show the extra deposited material around final geometry mode (including machine allowances). As can be seen in the left picture, the deposited part completely covers the final geometry. On the right, a cross-section view was set to illustrate the dimple the wall structure. Small amount of material covers the final geometry, however for the error from scanning and modelling alignment, we cannot be certain that this pit does not show in the final machined component

Wall thickness assessment concludes that wall thicknesses vary between 11 mm and 8,5 mm. This would result in average of 1,5 mm variation of surface height. Using parameter estimation from Fuchs *et al.* [57] would result in 1,875 mm machining allowance. In the outer wall we had 2 mm machining allowance, which seems to be barely enough. Therefore, based on scanned model and theoretical value (with our process parameters and setup) material allowance be 2 mm or more. However, if regional indentation caused by the dimple is excluded from the observation, our estimation would result in 1,25 mm machine allowance.

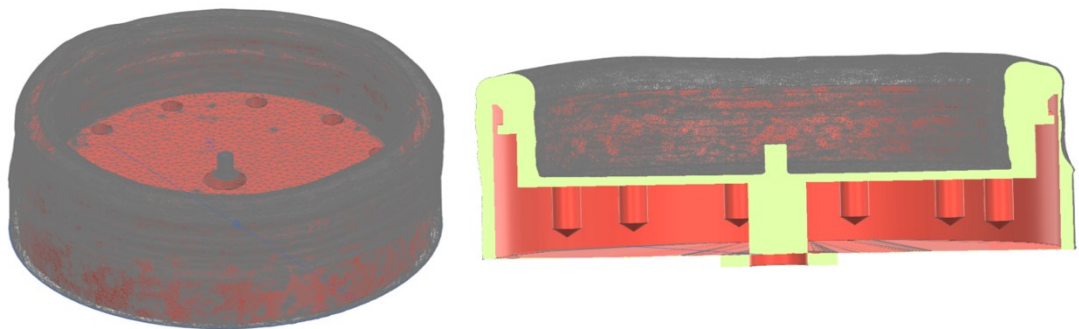


Figure 28. Deposited part as stock model (red colour: final model, grey colour: deposited model, greenish colour: extra deposited material including material allowance).

Post-processing was studied with two machining simulations. Machining simulations were conducted with Siemens NX CAM software. The first machining simulation was developed on the scanned model was used as a raw stock model, and the second simulation was performed on the full cylindrical raw stock. Machining was primarily executed by milling. Figure 29 illustrates different raw stock models, and the lost material percentage during post-processing. Material losses are calculated based on volume values estimated by NX.

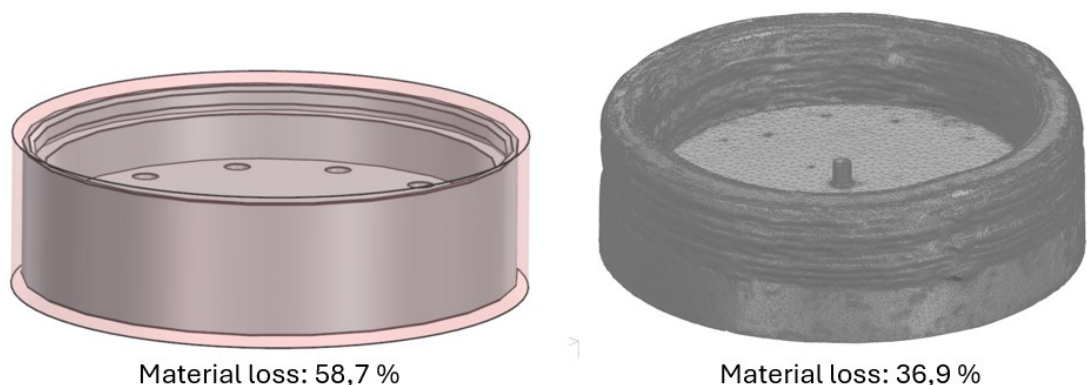


Figure 29. Comparison of material losses for two different inputs in machining simulation (left: Cylindrical raw stock, right: WAAM deposited component).

Simulations were run with equivalent values and same work operations were performed on both models. The main differences in tool paths came from cavity and outside wall millings. Based on the simulation both deposited raw stock and traditional raw stock can be machined without problems. Different machining values given by simulation are presented below in Table 7.

Table 7. Post-processing values of deposited and traditional block raw stocks in case study 1.

	Time (min)	Material loss (%)	Cutting length (mm)
Deposited raw stock	4:46	36,9	5145
Block raw stock	5:07	58,7	5134

Using deposited raw stock saves both time and material. However, cutting lengths are close to each other, and with deposited raw stock during the path less material is removed. Figure 28 shows that there is room for improvement in the deposited part. For example, inner cylinder surface seems to have extra material, of which could be eliminated. This would further improve deposited part as a raw stock part.

4.1.4 Machining post-processing

Two different parts were post-processed by machining. One of the parts was P3, had substrate diameters 100 mm and height of 14 mm. P3 is the same part that was scanned and used in geometry and simulation analyses. The other was smaller component P2, with substrate diameters of 96 mm and height of 14 mm.

First step of milling post-processing was to determine suitable fixing and the place of the origin in the work piece. Components fastening was challenging due to its shape. Since wall was deposited to the edge of the substrate and the whole wall (deposition + substrate) was going to be machined, there was little fastening surface. Therefore, specific soft jaws were fabricated for the 3-jaw chuck. This fastening system was used in determining the work origin in the middle of the component.

Same tools, machining parameters and much of the same program could be used in machining deposited part as in machining from the entire raw stock block. The difference came at the roughing state of the interior surface where milling the deposited part required less material removal due to its shape. If deposition geometry sufficient and there was enough machine allowance material, difference in machining a deposition compared to block was not noticed. In general, deposition component requires more setup and examination before machining.

Post-process machining of cycloid drive housing with WAAM + machining was successful. Among the two machined component, P3 (with larger diameter) exhibits a good result, shown in Figure 30. Final component did not leave any deposited surface visible, so we can conclude that machine allowance was adequate. Furthermore, coordinate alignment of two setups succeeded. In future we might improve our process by narrowing the wall. This could result in time, material, time and energy savings.

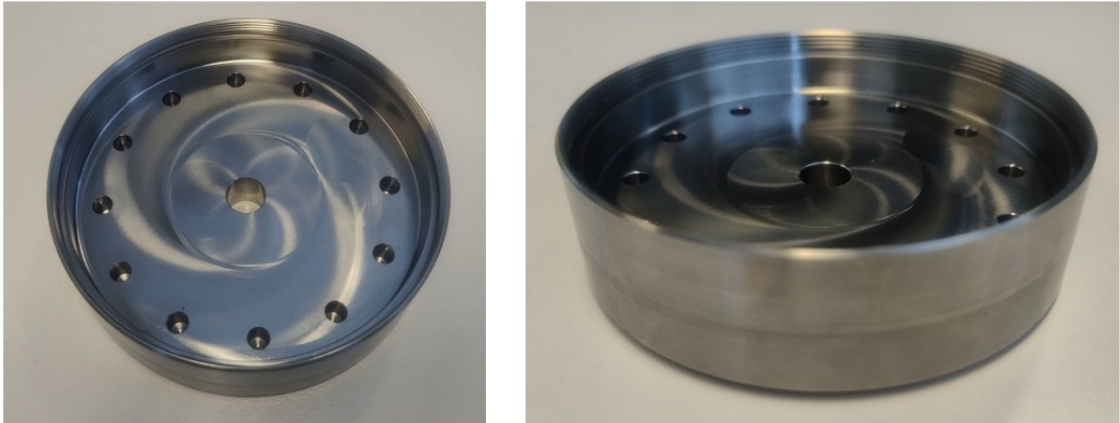


Figure 30. WAAM + machining result of P3 case 1.

Result of P2 part can be seen in Figure 31. After post-process, this part has several areas where deposition surface is visible. The entire inside as well as a large area on the outside wall is follows the desired geometry.

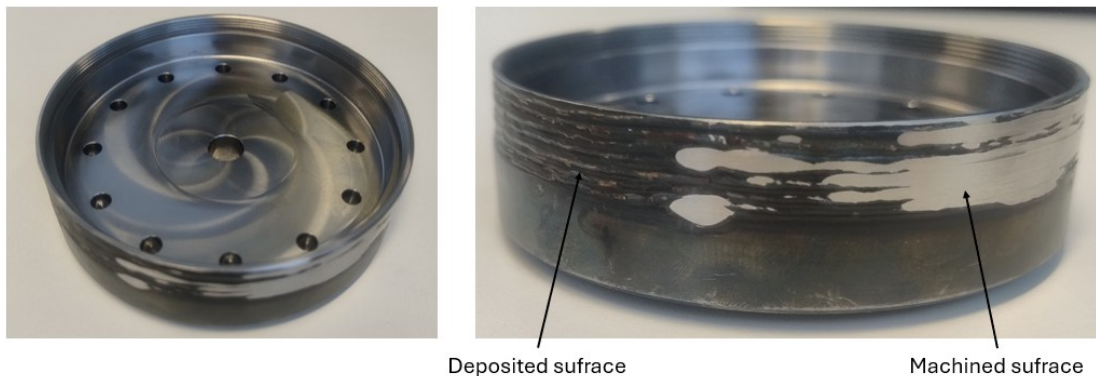


Figure 31. WAAM + machining result of P2 component.

The result of machining P2 indicates that the machining allowance was not evenly enough in the component. Even though there are some scatters places with enough machining allowance, majority of the regions in the component exhibits lack of machining allowance. The diameter of the substrate was same 96 mm as the outer wall of our final geometry. Therefore, to ensure sufficient machining allowance, there should have been minimum of 1,25 mm overhang, which might have resulted pouring/dropping the melted metal. Therefore, increasing substrate size and diameter of deposited cylinder is more

secure way of achieving desired results. Even if it leads to a greater amount of wasted material.

4.1.5 Evaluation of case 1

The focus of case 1 was to investigate WAAM + machining as an alternative manufacturing method to fabricate cycloid drive housings. In design phase, we predicted that geometry is possible to manufacture this way, however machining might be more effective option. After finalizing the test, we can confirm that WAAM + machining can be used as an alternative manufacturing method. Produced P2 cycloid drive housing is equivalent to a purely machined part. Since the whole structure (deposited and substrate) was machined during post-processing, the part has same surface roughness, geometrical and dimensional tolerances as general machined component.

From manufacturing point of view, experimentally measured manufacturing time for WAAM + machined component is around 68 minutes (65 + 3) of which most is spent in interlayer cooling, and setups. Arc-on time and machining time are combined only 15 minutes. In comparison, estimated time on purely machining the part around five minutes. Machining this component is the most efficient choice for production cases where batch sizes are relatively large. However, as a small-scale production component (e.g. custom design components), the profitability of WAAM + machining manufacturing method grows since futile arc-off time decreases since one part can be fabricated while other cools down. It should be noted that the size of the component and level of complexity are influencing factors for drawing this conclusion.

The deposition of each part takes 65 minutes, however arc-on time is only a little bit over 12 minutes. By depositing more pieces at the same time, WAAM setups utilization rate is increased. Thus, multiple parts could be fabricated simultaneously, utilizing fully other parts interlayer cooling time. Producing five components would take almost as little time as producing one. Production time of WAAM + machining and pure machining in relation to small-batch size is illustrated in Figure 32. In production times only arc-on time and machining times are perceived, illustrating circumstances where both machine setups would run on 100% utilization rate. Setup and preparation times are assumed to be similar and therefore can be left out of scope. In the graph blue curve represents the WAAM + machining production and red line machined production. Since the curves can be expected to continue linearly, we can state that case 1 is more efficient to produce by machining regardless of batch size. From WAAM + machining, we can observe the change in the curve in the 5-component batch size. This is when this geometry's arc-on time is fully utilized.

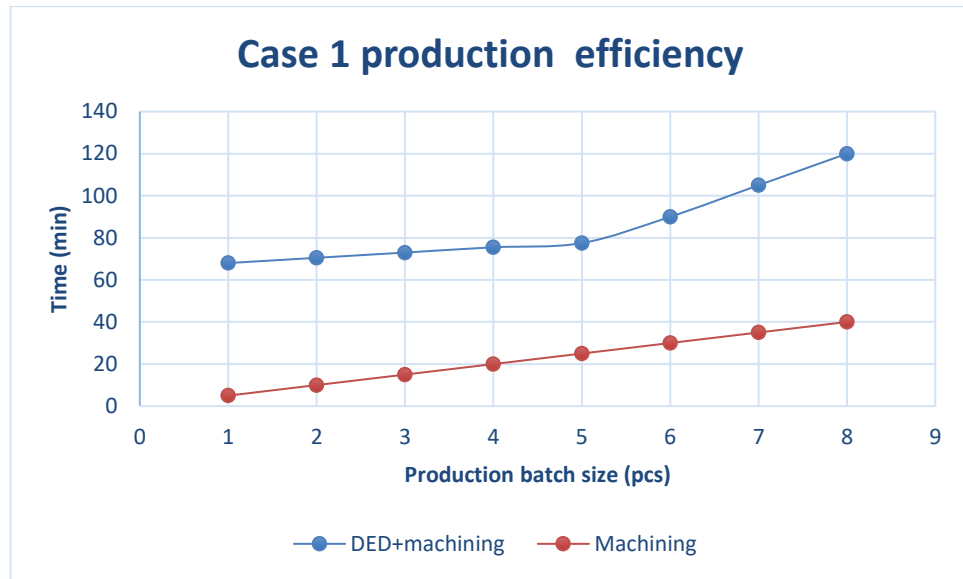


Figure 32. A Graph of case 1 production efficiency of different manufacturing methods.

An estimate of cost was calculated using Life Cycle Costing (LCC) method. Values for significant cost element data was drawn from literature ([62], [63]) and cost structure of case one was calculated using measured values from Table 5. The total cost of manufacturing case 1 part was estimated to be 44 €. More detailed description of cost distribution is illustrated in Figure 33.

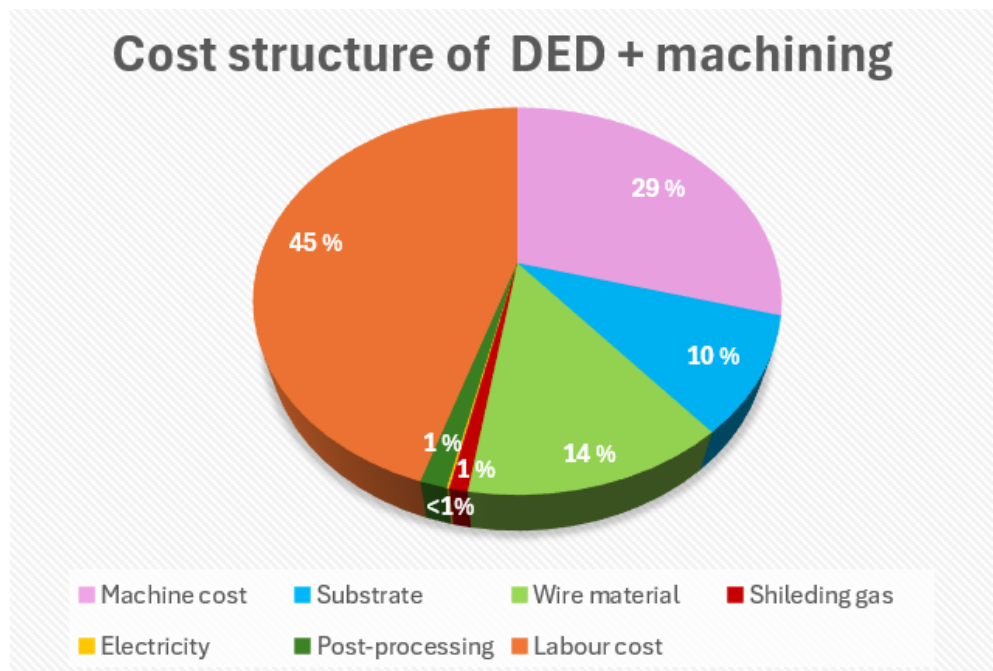


Figure 33. Cost structure of case study 1, total cost: 44 €.

The labour cost is the biggest contributor for the cost. Second biggest factor is machine cost, and material costs come only in third. As previously stated, cost analyses for WAAM

contains a lot of variety. For example, Kokare *et al.* [64] produced similar cylindrical geometry. In their results most of cost was due to post-processing, then labour and third biggest factor was machine cost. Thus, labour and machine costs tend to be greater cost contributors. However, further development of WAAM is most likely to bring production costs down in the future, when for example, manual supervision of the whole process can be eliminated [59]. Kokare *et al.* [64], also discussed the effect of batch size to production cost in their study. They estimated costs to decrease significantly in small-scale production. Figure 34 illustrates the graph they presented in their study. The cost of case 1 part is added in the figure with red dot. According to this study, by increasing the production batch size, cost per unit would be reduced significantly. In batch sized over three, hybrid WAAM would be more economical choice compared to machining.

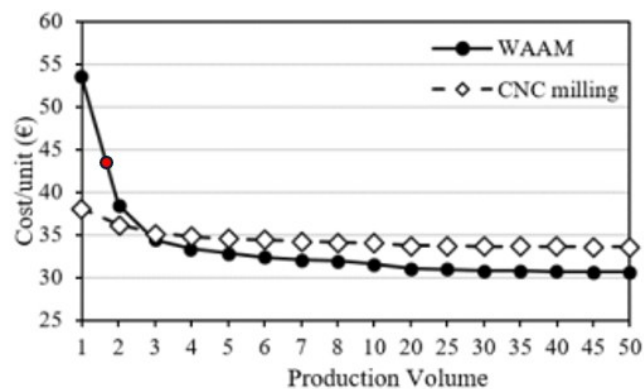


Figure 34. Cost per unit in relation to production volume [64].

Previously we stated that the sustainability of the component is affected by number of different characteristics, such as material efficiency, geometry, material, size and so on. Case 1 geometry is rather small in the scale of WAAM components and has a simple geometry. These aspects might indicate in sustainability point of view, WAAM comes in second to machining. By calculating manufacturing material efficiencies for WAAM + machining and purely machining for case 1, we can study the sustainability aspect. Manufacturing material efficiency is calculated by comparing the final mass of the product to the mass of consumed raw material [59]. WAAM + machining had material efficiency of 55,3 % and machining had lower value of 41,3 %. According to Kokare *et al.* [62] alternation in manufacturing material efficiency does not affect much WAAM, but it stays steadily around 1000 mPts of environmental impact. Machining however has descending linear curve, indicating decreasing environmental impact when material efficiency percentage grows. Breakeven point is around 25 %, of which both case 1 values are. This would indicate that that both manufacturing methods have relatively low environmental impact, but machining is ecologically better choice.

Therefore, from a sustainability perspective in Case 1, the choice between hybrid WAAM and machining has minimal impact. But from those two, machining is slightly better. By changing the geometry to more complex, increasing solid-to-cavity ratio or by increasing the size, relative sustainability of WAAM component would increase, and could made hybrid WAAM more desirable option. Especially, considering that most of the emissions come from material formation and WAAM can optimize material consumption. Nevertheless, since no in-depth LCA study has been conducted, and instead the results have been compared to existing literature, no precise conclusion could be drawn in this regard.

4.2 Manufacturing case study 2

WAAM + machining in the scope of 2,5D components was studied by manufacturing case study 2. Furthermore, known to be challenging features for overlapping deposition method were fabricated as well as a weaving deposition method feature. A digital scan model was built to study the geometrical accuracy, distortions and overall success of case 2 manufacturing. Lastly, utilization of primitive geometry, fabrication of designed part and ability form different features were evaluated. Based on results topics for further research was proposed.

4.2.1 Deposition of case study 2

Steel (S355) plate with dimension of 280 x150 x11 mm was used as substrates. The substrates were brushed with steel brush to ensure the grip of first layers. Similar process parameters were used: wire-feed rate of 4 m/mm, welding travel speed of 8 mm/s, shielding gas contained 18 % CO₂ and 82 % Ar. First build up deposition had 13 layers and fabricated contour wall, four wedge features, and all platform features. In addition to the transition time of the robot arm, we had a 5-second wait time between each arc-extinguish and arc-ignite. Interlayer temperatures were maintained under 200 degrees Celsius. The time of each round and of the entire deposition was measured and is shown in Table 8.

Table 8. Illustration of different layer deposition times (deposition time decreases due to lessened feature deposition as layers increase).

Layer	1	2	3	4	5	6	7	8	9	10	11	12	13	Sum
Time (min)	8,5	8,5	9,3	6,3	6,3	6,4	6,4	2,3	2,1	2,1	2,1	1,4	1,3	65,05

After first build up deposition the cylindric feature was deposited using weaving deposition path. Used weaving shape was zig-zag pattern, where nozzle moves only in X, Y - coordinate system and Z value remains as zero. Deposition was concluded with adequate proven process parameters for weaving, wire-feed rate was 4 m/min, welding speed 2,5 mm/s, weave length was 2 mm, amplitude 5 mm and used shielding gas contained 18 % CO₂ and 82 % Ar. Seven layers were printed, with 2,5 mm layer height. Each weave layer took 65,5 seconds to print, and arc-on time of whole feature was 7 minutes and 34 seconds. Both depositions were deemed as successful, and results are illustrated in Figure 35.



Figure 35. Result of deposition of case study 2.

Visually, all features were printed as planned, and no significant defects were detected during built up, which might have remained inside structure causing its deterioration.

However, a clear deflection can be observed in the substrate due to the heat input and size of the substrate.

From this size part, we can clearly assess if deposited part has defect typical to used material. According to Figure 4 steel as a WAAM material is prone to poor surface finish, deformation and residual stresses and cracking. From these defects, poor surface finish and deformation can be seen clearly from the deposited part. Additionally, some spatter can be noted.

4.2.2 Component scan and machining simulation

For further analysis the produced geometry was scanned and reworked into a digital 3D format. Point cloud was formed and worked in PolyWorks Inspector and revised into solid 3D part in Siemens NX CAD software. The scan of the component is illustrated in Figure 36 (left). Figure 36 also presents the deposited geometry and redesigned primitive shape geometries on top of each other's in right figure. Deposited and scanned geometry is presented as a grey colour a primitive geometry model is displayed in red colour.

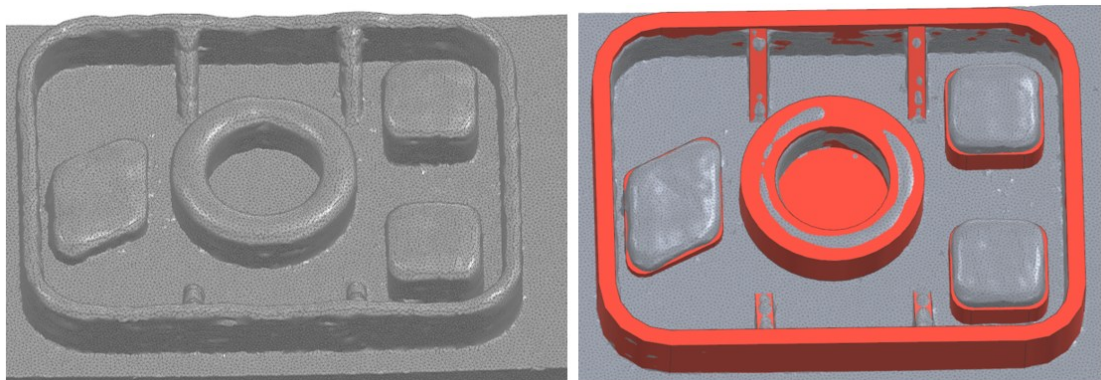


Figure 36. Scanned deposition geometry and comparison with primitive shape geometry model.

If the deposited geometry had matched the redesigned model fully, we would only see grey coloured areas. However, produced contour wall does not reach intended wall height in any point, and intended wall width only in some areas. Interestingly, deposition covers more area in the inside of the wall than outside. Three platform features are each higher than intended, but lack in perimeter. Wedge features seem to come closest to the design dimensions. Cylindric feature have adequate dimensions, both in height and width directions. Successive models also display the deflection of the substrate, since the deposited substrate is visible elsewhere that in the middle, where is has bend of the substrate is so notable that redesigned model is visible. Nonetheless, it was known that the WAAM component would not fully match the designed geometry. Therefore, we also compare the deposited component with final geometry model. From Figure 37 we can

see final geometry model submerged in scanned deposition model. In the left side picture, the red colour is the final geometry model, and scanned deposition is grey coloured. In the right-side picture, grey colour displays the deposition substrate, greenish colour displays places without overlapping models and red colour illustrated the overlapping models. Since we could detect the red colour of submerged final geometry model there was not enough material to form the final component.

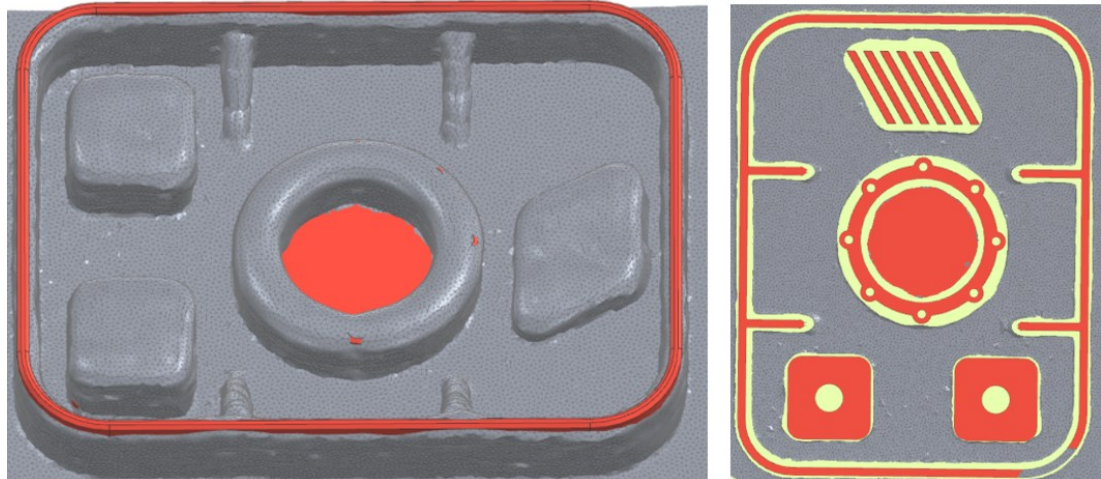


Figure 37. Successive scanned deposition model and final geometry model (red colour: final model, grey colour: deposited model, greenish colour: extra deposited material including material allowance).

The focus of this second case study was to investigate the fabrication of different features. Therefore, we next observe each deposited feature separately. The final geometry contour wall is fully embedded into deposited model in width direction but is not in height. By changing the wall geometry in NX we can observe that the deposited contour falls short 1-3 mm. Highest points of the contour wall are in the wedge intersection, since more material piles up on there. In some places there is little material for machining allowance, nevertheless the whole wall is covered by deposited material. Therefore, we can assume that post-process machining would be successful.

Wedge features and intersection appear to have formed properly. Intersections are challenging due to material pile up but based on Figure 37, every wedge feature have adequate amount of material surrounding them. Furthermore, more detailed figures from deposited features are collected in Figure 38. From there we can see a cross-section of wedge features (c), which can be used to ensure enough deposition material in all surfaces to form this feature.

Rib feature platform has enough material in X, Y -directions, though barely in two corners. From the cross-section view we can observe the amount of material in Z -directions, which is defined by layer height. In Z -direction there seems to be almost double the

amount of material needed. This feature was formed with three layers but could have probably been made with only two layers, to avoid unnecessary material waste.

Similar occurrence can be seen with other platform features (cube and cylinder). In X, Y -directions, features are fully covered by deposition but here and there material allowance might be too slim. However, in Z -direction there is a lot of extra material. This feature could also have been formed with fewer number of layers. This also highlights an importance of online monitoring system to evaluate the deposited geometry during the print.

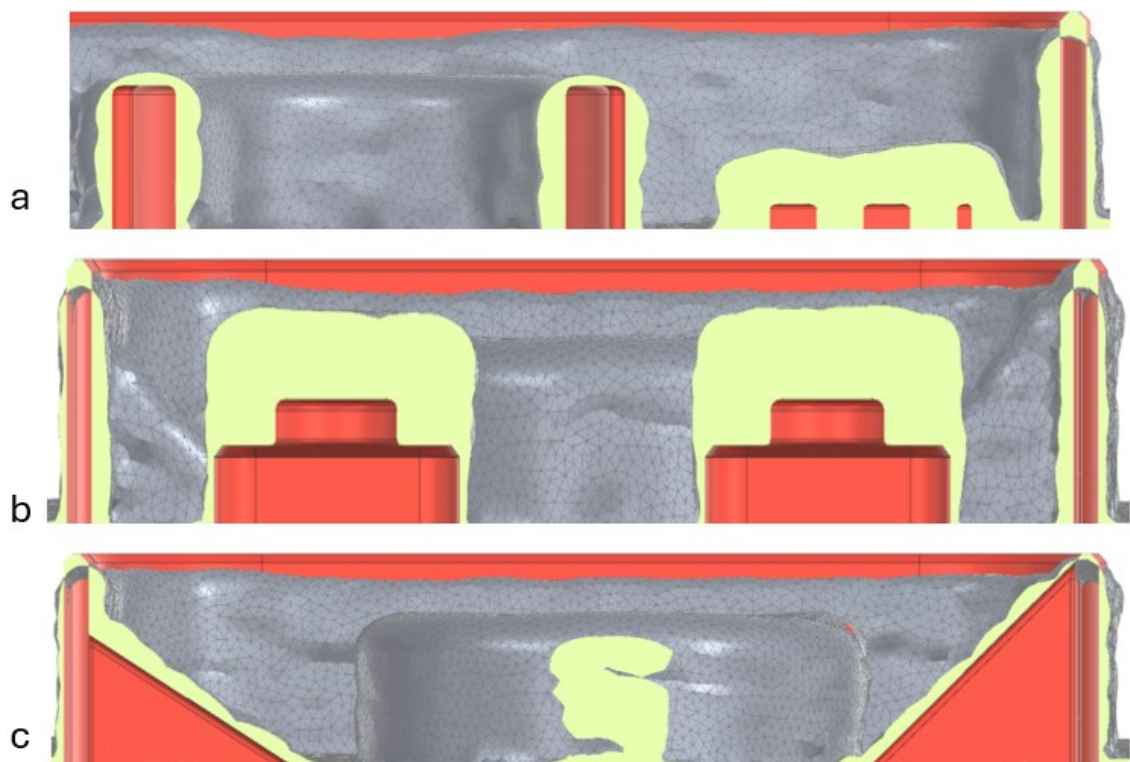


Figure 38. Three cross-section view of deposited features.

Cylinder feature, deposited with weaving strategy, has sufficient size in X, Y-directions. Both inside and outside walls seem to have satisfactory machining allowances. However, in Z -direction the height is not enough in couple of places, which has red colour shining through. Unfortunately, the curved surface of the deposition layer enhances this issue. Overall, all features were formed successfully with WAAM, even though there was unpredictability and inaccuracies in the dimensions.

Post-processing was studied with NX Siemens CAM simulations. One simulation was conducted with scanned model of case 2 as a raw stock model and the other with bounding box extrusion raw stock. See illustration of input raw stacks and their material losses from Figure 39. Machining was executed by milling. Simulations were run with equivalent

values and same work operations were performed on both models. The main differences in tool paths came from cavity and outside wall millings.

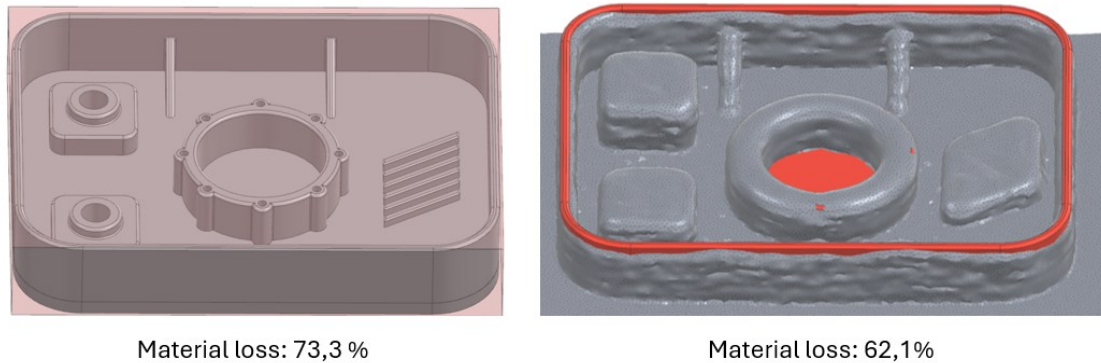


Figure 39. Comparing different material losses and different raw stocks in machining simulation (left: block raw stock, right: WAAM deposited raw stock).

Based on these simulations both traditional raw stock and deposited raw stock models can be machined successfully. Though due to insufficient deposition height in some areas, final model could not be fully produced from deposited raw stock model. However, these shortcomings did not affect the simulation. Different machining values given by simulation are presented below in Table 9.

Table 9. Post-process machining values for deposited and traditional raw stock models in case study 2.

	Time (min)	Material loss (%)	Cutting length (mm)
Deposited raw stock	10:46	62,1	21391
Block raw stock	13:21	73,3	32970

Deposited raw stock required less machining time and shorter cutting length. Furthermore, material loss is smaller even though substrate was included in the calculations. From Figure 38 illustrates the amount of extra deposition material in certain features. By eliminating this extra material would further improve machining deposited raw stock part.

4.2.3 Evaluation of case study 2

The purpose of case study 2 was to investigate WAAM manufacturing by fabricating different features in 2,5D component. Some features were common challenging features for WAAM, and others were modelled after typical features found in engine housings. Due to limitation in geometrical accuracy and surface finish, WAAM is combined with

post-process machining to produce functioning surfaces. Deposition process was simplified by using primitive geometries in redesigning phase. Machining post processing was studied with Siemens NX CAM simulation in this case instead of actual machining.

Designed features and 2,5D geometry can be manufactured with WAAM with ease. Production process was simple and relatively fast and fabricated part could be used as a post-processing raw stock. Furthermore, significant material savings could be achieved even when substrate was included in material loss calculations. However, some shortcomings could be observed from the deposition: contour wall and cylindric features were not built up to height successfully. Additionally, platform features had plentiful of extra material, which lead to unnecessary material waste. Therefore, room for improvement was left in fabricating case study 2, and therefore subsequent deposition could be advantageous in further research.

Unsuccessful fabrication of overlap features was caused by faulty or incomplete understanding of material behaviour during build up. One contributing factor could also be too high interlayer temperature, which affects the height of the bead geometry. In the design phase, there was an assumption of general 2 mm step up height for each layer, of which basis the design was sliced into deposition layers. However, contour layers were less than and platform feature layers were over 2 mm, resulting in unpredicted heights for some features. Different realized and estimated layer heights are elaborated in Table 10.

Table 10. Comparing true and estimated layer heights.

	Designed layer height (mm)	Average layer height in reality (mm)	Number of deposited layers (pcs)	Optimized number of layers (pcs)
Rib feature	2	2,7	3	2
Wedge features	2	2	Lower 8, Higher 11	Lower 8, Higher 11
Contour wall	2	1,7	13	16
Raised platform / tube features	2	2,7	7	5
Cylindric feature	2,5	2,4	7	8

Thus, to make design processing for deposition and thereafter programming uncomplicated, material behaviour during deposition should be considered in primitive geometry designing. Based on case study 2, single bead constructions should have at least 20% added wall height and filled platform structures should have 35% decrease in height. Furthermore, the width and length of each platform feature should be increased slightly. By improving the deposited part accuracy, we improve the utilization of WAAM. In addition, we can reduce material waste and build up time (~10%) which improve sustainability. However, these values are based on one case study and one deposition, and to verify these conclusions, additional investigations must be conducted. Different process parameters, material or size of the features might for example, might affect the results.

The motivation behind improving primitive shape redesign is intricate. By utilizing primitive shapes in WAAM + machining manufacturing any complex structures can be produced with simple process steps. Furthermore, this simplification process improves WAAM general usability, reduces the workload of redesign and accelerate the production process. However, further investigation must be performed to form a functional primitive geometry arsenal with certified and predictable geometries. In this study we used only most basic primitive shape geometries, but employing more shapes or using combinations could result in closer near-net-shape component. Another interesting further investigation is the possibility of automation in WAAM + machining processes when utilizing primitive geometries.

5. SUMMARY AND CONCLUSIONS

WAAM has great potential and therefore has garnered a lot of attention recently in manufacturing large components. It is an appealing manufacturing method due to its ability to fabricate components with high manufacturing efficiency and low production cost. Furthermore, it is a serious competitor to traditional manufacturing methods since it can produce valuable structural parts with fewer material losses and often in shorter times. WAAM's high deposition rate and high heat input is what makes its production fast. However, it also contributes to the WAAM's greatest challenges and impediments, geometrical distortions, large feature sizes, and high surface waviness/roughness. One solution to this complication is to combine WAAM and machining. WAAM + machining manufacturing can be fast, ecological and achieve desirable surface roughness and geometrical precision. Unfortunately, this can be a challenging task and there is still much to investigate in combined WAAM + machining manufacturing method. Furthermore, a significant information gap can be found between manufacturing investigations and fully utilizing WAAM + machining opportunities in production. Primary objective of this thesis is to investigate WAAM + machining manufacturing method on the above-mentioned information gap.

Two experimental studies have been conducted in this thesis. Key findings from case study 1 investigation indicate that WAAM + machining is a feasible alternative manufacturing method for traditional manufacturing. Benefits of utilizing this hybrid manufacturing method include reduced machining time, machining length and affordable production cost when comparing to machined component. However, machining was better choice ecologically and had better production efficiency regardless of batch size. Case study 2 indicated that through primitive geometries complex geometries can be fabricated. Furthermore, WAAM + machining manufacturing can be simplified achieve efficient and uncomplicated production process. Implication of these findings are promising. Combination of WAAM + machining manufacturing methods provides a noteworthy option for traditional manufacturing. Although WAAM is not best production method for every existing geometry, it should be kept in mind as a viable alternative, as it has variety of advantages from freedom of design known in additive manufacturing design and precision and high quality inherent in machining.

Some limitations should be acknowledged. Investigations were performed with one material and one set of process parameters, and results might vary with of different values. Furthermore, this thesis focused only on small 2,5D geometries and therefore results

cannot be applied to all geometries. The sample size of the thesis was also small. Future research should focus on advancing primitive shape geometry redesign to improve the material efficiency of the component as well as to simplify the WAAM + machining manufacturing process. This could advance the full utilization of this manufacturing method in industrial production. Furthermore, extensive LCA analysis should be performed to fully understand the ecological implications of this hybrid manufacturing method. In conclusion, hybrid WAAM + machining manufacturing can produce geometrically accurate high value part fast and ecologically. Throughout different industries, WAAM + machining deserves to be adapted as part of everyday design and manufacturing.

REFERENCES

- [1] H. A. Abdel-Aal, *Additive Manufacturing of Metals: Fundamentals and Testing of 3D and 4D Printing*, 1st Edition. McGraw-Hill Education, 2022. Accessed: Jan. 16, 2025. [Online]. Available: <https://www.accessengineeringlibrary.com/content/book/9781260464344>
- [2] N. Knezovic and B. Dolšak, 'In-process non-destructive ultrasonic testing application during wire plus arc additive manufacturing', *Adv. Prod. Eng. Manag.*, vol. 13, no. 2, pp. 158–168, 2018, doi: 10.14743/apem2018.2.281.
- [3] L. P. Raut and R. V. Taiwade, 'Wire Arc Additive Manufacturing: A Comprehensive Review and Research Directions', *J. Mater. Eng. Perform.*, vol. 30, no. 7, pp. 4768–4791, 2021, doi: 10.1007/s11665-021-05871-5.
- [4] A. Shah, R. Aliyev, H. Zeidler, and S. Krinke, 'A Review of the Recent Developments and Challenges in Wire Arc Additive Manufacturing (WAAM) Process', *J. Manuf. Mater. Process.*, vol. 7, no. 3, 2023, doi: 10.3390/jmmp7030097.
- [5] H. Lockett, J. Ding, S. Williams, and F. Martina, 'Design for Wire + Arc Additive Manufacture: design rules and build orientation selection', *J. Eng. Des.*, vol. 28, no. 7–9, pp. 568–598, Sep. 2017, doi: 10.1080/09544828.2017.1365826.
- [6] O. C. Ozaner, D. Klobčar, and A. Sharma, 'Machining Strategy Determination for Single- and Multi-Material Wire and Arc Additive Manufactured Thin-Walled Parts', *Materials*, vol. 16, no. 5, p. 2055, Mar. 2023, doi: 10.3390/ma16052055.
- [7] L. K. Gillespie, Ed., *Design for Advanced Manufacturing: Technologies and Processes*, 1st Edition. McGraw-Hill Education, 2017. Accessed: Jan. 16, 2025. [Online]. Available: <https://www.accessengineeringlibrary.com/content/book/9781259587450>
- [8] B. M. Bidanda, Ed., *Maynard's Industrial and Systems Engineering Handbook*, 6th Edition. McGraw-Hill Education, 2023. Accessed: Jan. 16, 2025. [Online]. Available: <https://www.accessengineeringlibrary.com/content/book/9781260461565>
- [9] F. Li, S. Chen, J. Shi, H. Tian, and Y. Zhao, 'Evaluation and optimization of a hybrid manufacturing process combining wire arc additive manufacturing with milling for the fabrication of stiffened panels', *Appl. Sci. Switz.*, vol. 7, no. 12, 2017, doi: 10.3390/app7121233.
- [10] H. J. Son, B. W. Seo, C. J. Kim, S. Kim, and Y. T. Cho, 'Coordinate system setting for post-machining of impeller shape by wire arc DED and evaluation of processing efficiency', *Sci. Rep.*, vol. 14, no. 1, 2024, doi: 10.1038/s41598-024-68723-x.
- [11] D. Ding, Z. Pan, D. Cuiuri, and H. Li, 'Wire-feed additive manufacturing of metal components: technologies, developments and future interests', *Int. J. Adv. Manuf. Technol.*, vol. 81, no. 1–4, pp. 465–481, 2015, doi: 10.1007/s00170-015-7077-3.
- [12] R. Sarma, S. Kapil, and S. N. Joshi, 'Build Strategies Based on Substrate Utilization for 3-Axis Hybrid Wire Arc Additive Manufacturing Process', *Adv. Mater. Sci. Eng.*, vol. 2022, 2022, doi: 10.1155/2022/4988301.
- [13] S. M. Yusuf, S. Cutler, and N. Gao, 'Review: The impact of metal additive manufacturing on the aerospace industry', *Metals*, vol. 9, no. 12, 2019, doi: 10.3390/met9121286.
- [14] H. Pant, A. Arora, G. S. Gopakumar, U. Chadha, A. Saeidi, and A. E. Patterson, 'Applications of wire arc additive manufacturing (WAAM) for aerospace component manufacturing', *Int. J. Adv. Manuf. Technol.*, vol. 127, no. 11–12, pp. 4995–5011, 2023, doi: 10.1007/s00170-023-11623-7.
- [15] B. Wu *et al.*, 'A review of the wire arc additive manufacturing of metals: properties, defects and quality improvement', *J. Manuf. Process.*, vol. 35, pp. 127–139, 2018, doi: 10.1016/j.jmpro.2018.08.001.
- [16] D. Ashok and M. V. A. R. Bahubalendruni, 'Design and Characterization of 2.5D Nature-Inspired Infill Structures under Out-Plane Quasi-Static Loading Condition', *Adv. Mater. Sci. Eng.*, vol. 2023, no. 1, p. 8918937, 2023, doi: 10.1155/2023/8918937.
- [17] S. I. Evans, J. Wang, J. Qin, Y. He, P. Shepherd, and J. Ding, 'A review of WAAM for steel construction – Manufacturing, material and geometric properties, design, and future directions', *Structures*, vol. 44, pp. 1506–1522, 2022, doi: 10.1016/j.istruc.2022.08.084.

- [18] J. Liu, Y. Xu, Y. Ge, Z. Hou, and S. Chen, 'Wire and arc additive manufacturing of metal components: a review of recent research developments', *Int. J. Adv. Manuf. Technol.*, vol. 111, no. 1–2, pp. 149–198, 2020, doi: 10.1007/s00170-020-05966-8.
- [19] V. Laghi, N. Babovic, E. Benvenuti, and H. Kloft, 'Blended structural optimization of steel joints for Wire-and-Arc Additive Manufacturing', *Eng. Struct.*, vol. 300, 2024, doi: 10.1016/j.engstruct.2023.117141.
- [20] H. Nagamatsu, H. Sasahara, Y. Mitsutake, and T. Hamamoto, 'Development of a cooperative system for wire and arc additive manufacturing and machining', *Addit. Manuf.*, vol. 31, p. 100896, Jan. 2020, doi: 10.1016/j.addma.2019.100896.
- [21] B. Ahmad, X. Zhang, H. Guo, M. E. Fitzpatrick, L. M. S. C. Neto, and S. Williams, 'Influence of Deposition Strategies on Residual Stress in Wire + Arc Additive Manufactured Titanium Ti-6Al-4V', *Metals*, vol. 12, no. 2, 2022, doi: 10.3390/met12020253.
- [22] C. Zhang, Z. Li, J. Zhang, H. Tang, and H. Wang, 'Additive manufacturing of magnesium matrix composites: Comprehensive review of recent progress and research perspectives', *J. Magnes. Alloys*, vol. 11, no. 2, pp. 425–461, 2023, doi: 10.1016/j.jma.2023.02.005.
- [23] M. Wieczorowski, A. Pereira, D. Carou, B. Gapinski, and I. Ramirez, 'Characterization of 5356 Aluminum Walls Produced by Wire Arc Additive Manufacturing (WAAM)', *Materials*, vol. 16, no. 7, p. 2570, Mar. 2023, doi: 10.3390/ma16072570.
- [24] M. Rauch, J.-Y. Hascoet, and V. Querard, 'A multi-axis tool path generation approach for thin wall structures made with waam', *J. Manuf. Mater. Process.*, vol. 5, no. 4, 2021, doi: 10.3390/jmmp5040128.
- [25] J. S. Panchagnula and S. Simhambhatla, 'Manufacture of complex thin-walled metallic objects using weld-deposition based additive manufacturing', *Robot. Comput.-Integr. Manuf.*, vol. 49, pp. 194–203, 2018, doi: 10.1016/j.rcim.2017.06.003.
- [26] J. Müller and J. Hensel, 'WAAM of structural components—building strategies for varying wall thicknesses', *Weld. World*, vol. 67, no. 4, pp. 833–844, 2023, doi: 10.1007/s40194-023-01481-y.
- [27] L. Nguyen, J. Buhl, and M. Bambach, 'Multi-bead overlapping models for tool path generation in wire-arc additive manufacturing processes', presented at the Procedia Manufacturing, 2020, pp. 1123–1128. doi: 10.1016/j.promfg.2020.04.129.
- [28] D. Ding, Z. Pan, D. Cuiuri, and H. Li, 'A multi-bead overlapping model for robotic wire and arc additive manufacturing (WAAM)', *Robot. Comput.-Integr. Manuf.*, vol. 31, pp. 101–110, Feb. 2015, doi: 10.1016/j.rcim.2014.08.008.
- [29] Y. Cao, S. Zhu, X. Liang, and W. Wang, 'Overlapping model of beads and curve fitting of bead section for rapid manufacturing by robotic MAG welding process', *Robot. Comput.-Integr. Manuf.*, vol. 27, no. 3, pp. 641–645, Jun. 2011, doi: 10.1016/j.rcim.2010.11.002.
- [30] Z. Hu, X. Qin, Y. Li, J. Yuan, and Q. Wu, 'Multi-bead overlapping model with varying cross-section profile for robotic GMAW-based additive manufacturing', *J. Intell. Manuf.*, vol. 31, no. 5, pp. 1133–1147, 2020, doi: 10.1007/s10845-019-01501-z.
- [31] Q. Guo *et al.*, 'Design and validation of 3D self-supporting structures and printing paths for multi-axis additive manufacturing', *Addit. Manuf.*, vol. 96, 2024, doi: 10.1016/j.addma.2024.104563.
- [32] J. Zhao *et al.*, 'Influence of deposition path strategy on residual stress and deformation in weaving wire-arc additive manufacturing of disc parts', *J. Mater. Res. Technol.*, vol. 30, pp. 2242–2256, 2024, doi: 10.1016/j.jmrt.2024.03.226.
- [33] A. Suárez, P. Ramiro, F. Veiga, T. Ballesteros, and P. Villanueva, 'Benefits of Aeronautical Preform Manufacturing through Arc-Directed Energy Deposition Manufacturing', *Materials*, vol. 16, no. 22, p. 7177, Nov. 2023, doi: 10.3390/ma16227177.
- [34] G. Ma, G. Zhao, Z. Li, and W. Xiao, 'A Path Planning Method for Robotic Wire and Arc Additive Manufacturing of Thin-Walled Structures with Varying Thickness', presented at the IOP Conference Series: Materials Science and Engineering, 2019. doi: 10.1088/1757-899X/470/1/012018.
- [35] X. Fu *et al.*, 'Flexible 2.5D Metamaterial with High Mechanical Bearing Capacity for Electromagnetic Interference Filters at Microwave Frequency', *Adv. Eng. Mater.*, vol. 22, no. 3, p. 1901126, 2020, doi: 10.1002/adem.201901126.
- [36] 'Moottorikotelo', Ningbo Yinzhou Kuangda Trading Co., Ltd. Accessed: Jan. 16, 2025. [Online]. Available: <http://fi.metallecas.com/motor-housing.html>
- [37] Y. Wang, D. Wang, S. Zhang, Z. Tang, L. Wang, and Y. Liu, 'Design and development of a five-axis machine tool with high accuracy, stiffness and efficiency for aero-engine casing

- manufacturing', *Chin. J. Aeronaut.*, vol. 35, no. 4, pp. 485–496, Apr. 2022, doi: 10.1016/j.cja.2021.04.001.
- [38] L. Magerramova *et al.*, 'Design, simulation and optimization of an additive laser-based manufacturing process for gearbox housing with reduced weight made from als10mg alloy', *Metals*, vol. 12, no. 1, 2022, doi: 10.3390/met12010067.
- [39] L. Papadakis and C. Hauser, 'Experimental and computational appraisal of the shape accuracy of a thin-walled vireole aero-engine casing manufactured by means of laser metal deposition', *Prod. Eng.*, vol. 11, no. 4–5, pp. 389–399, 2017, doi: 10.1007/s11740-017-0746-3.
- [40] A. Addison, J. Ding, F. Martina, H. Lockett, and S. Williams, 'Manufacture of Complex Titanium Parts using Wire+Arc Additive Manufacture', in *Manufacture of Large Scale Aircraft parts*, Birmingham, United Kingdom: Cranfield University, May 2015.
- [41] X. Wang, W. Ding, and B. Zhao, 'A review on machining technology of aero-engine casings', *J. Adv. Manuf. Sci. Technol.*, vol. 2, no. 3, 2022, doi: 10.51393/j.jamst.2022011.
- [42] R. A. Walsh, 'Castings, Moldings, Extrusions, and Powder-Metal Technology', in *McGraw-Hill Machining and Metalworking Handbook*, 3rd Edition., McGraw-Hill Education, 2006. Accessed: Feb. 14, 2025. [Online]. Available: <https://www.accessengineeringlibrary.com/content/book/9780071457873/chapter/chapter12>
- [43] L. V. Whiting, 'Introduction', in *Principles of Metal Casting*, M. Sahoo and S. 'Sam' Sahu, Eds., McGraw-Hill Education, 2014. Accessed: Feb. 14, 2025. [Online]. Available: <https://www.accessengineeringlibrary.com/content/book/9780071789752/toc-chapter/chapter3/section/section2>
- [44] R. A. Walsh, 'Modern Metalworking Machinery, Tools, and Measuring Devices', in *McGraw-Hill Machining and Metalworking Handbook*, 3rd Edition., McGraw-Hill Education, 2006. Accessed: Feb. 20, 2025. [Online]. Available: <https://www.accessengineeringlibrary.com/content/book/9780071457873/chapter/chapter1>
- [45] J. G. SCHERER, 'CNC Control', in *Manufacturing Engineering Handbook*, 2nd Edition., H. Geng, Ed., McGraw-Hill Education, 2016. Accessed: Feb. 21, 2025. [Online]. Available: <https://www.accessengineeringlibrary.com/content/book/9780071839778/chapter/chapter10>
- [46] H. B. Kief and H. A. Roschiwal, *CNC Handbook*, 1st Edition. McGraw-Hill Education, 2012. Accessed: Jan. 16, 2025. [Online]. Available: <https://www.accessengineeringlibrary.com/content/book/9780071799485>
- [47] L. M. Alves and P. A. F. Martins, 'Flexible forming tool concept for producing crankshafts', *J. Mater. Process. Technol.*, vol. 211, no. 3, pp. 467–474, 2011, doi: 10.1016/j.jmatprotec.2010.10.024.
- [48] S. K. Mishra, S. P. R. S. S. Sajin Jose, and R. K. Upadhyay, 'Wire arc additive manufacturing: materials, processes and its constraints', *Mater. Manuf. Process.*, vol. 40, no. 6, pp. 723–740, Apr. 2025, doi: 10.1080/10426914.2025.2469525.
- [49] A. S. Yildiz, K. Davut, B. Koc, and O. Yilmaz, 'Wire arc additive manufacturing of high-strength low alloy steels: study of process parameters and their influence on the bead geometry and mechanical characteristics', *Int. J. Adv. Manuf. Technol.*, vol. 108, no. 11–12, pp. 3391–3404, 2020, doi: 10.1007/s00170-020-05482-9.
- [50] H. Wang, W. Jiang, J. Ouyang, and R. Kovacevic, 'Rapid prototyping of 4043 Al-alloy parts by VP-GTAW', *J. Mater. Process. Technol.*, vol. 148, no. 1, pp. 93–102, 2004, doi: 10.1016/j.jmatprotec.2004.01.058.
- [51] N. Chernovol, A. Sharma, T. Tjahjowidodo, B. Lauwers, and P. Van Rymentant, 'Machinability of wire and arc additive manufactured components', *CIRP J. Manuf. Sci. Technol.*, vol. 35, pp. 379–389, 2021, doi: 10.1016/j.cirpj.2021.06.022.
- [52] T. Abe, J. Kaneko, and H. Sasahara, 'Thermal sensing and heat input control for thin-walled structure building based on numerical simulation for wire and arc additive manufacturing', *Addit. Manuf.*, vol. 35, 2020, doi: 10.1016/j.addma.2020.101357.
- [53] F. R. Teixeira, V. L. Jorge, F. M. Scotti, E. Siewert, and A. Scotti, 'A Methodology for Shielding-Gas Selection in Wire Arc Additive Manufacturing with Stainless Steel', *Materials*, vol. 17, no. 13, 2024, doi: 10.3390/ma17133328.
- [54] F. Marefat, A. Kapil, S. A. Banaee, P. Van Rymentant, and A. Sharma, 'Evaluating shielding gas-filler wire interaction in bi-metallic wire arc additive manufacturing (WAAM) of creep resistant steel-stainless steel for improved process stability and build quality', *J. Manuf. Process.*, vol. 88, pp. 110–124, 2023, doi: 10.1016/j.jmapro.2023.01.046.
- [55] A. A. Kulikov, A. V. Sidorova, and A. E. Balanovskiy, 'Process Design for the Wire Arc Additive Manufacturing of a Compressor Impeller', presented at the IOP Conference Series: Materials Science and Engineering, 2020. doi: 10.1088/1757-899X/969/1/012098.

- [56] R. Reisch, T. Hauser, T. Kamps, and A. Knoll, 'Robot based wire arc additive manufacturing system with context-sensitive multivariate monitoring framework', presented at the Procedia Manufacturing, 2020, pp. 732–739. doi: 10.1016/j.promfg.2020.10.103.
- [57] C. Fuchs, D. Baier, T. Semm, and M. F. Zaeh, 'Determining the machining allowance for WAAM parts', *Prod. Eng.*, vol. 14, no. 5–6, pp. 629–637, 2020, doi: 10.1007/s11740-020-00982-9.
- [58] C. Fuchs, C. Fritz, and M. F. Zaeh, 'Impact of wire and arc additively manufactured workpiece geometry on the milling process', *Prod. Eng.*, vol. 17, no. 3, pp. 415–424, Jun. 2023, doi: 10.1007/s11740-022-01153-8.
- [59] K. Sommer, A. Pfennig, F. Sammler, M. Abdelmoula, D. Kamerer, and R. Heiler, 'First Approach in Analysis of Tool Wear When Milling Additive Manufacturing (AM) Parts', *Appl. Sci. Switz.*, vol. 14, no. 14, 2024, doi: 10.3390/app14146219.
- [60] R. Laue, P. Colditz, M. Möckel, and B. Awiszus, 'Study on the Milling of Additive Manufactured Components', *Metals*, vol. 12, no. 7, p. 1167, 2022, doi: 10.3390/met12071167.
- [61] P. C. Priarone, E. Pagone, F. Martina, A. R. Catalano, and L. Settineri, 'Multi-criteria environmental and economic impact assessment of wire arc additive manufacturing', *CIRP Ann.*, vol. 69, no. 1, pp. 37–40, 2020, doi: 10.1016/j.cirp.2020.04.010.
- [62] S. Kokare, J. P. Oliveira, T. G. Santos, and R. Godina, 'Environmental and economic assessment of a steel wall fabricated by wire-based directed energy deposition', *Addit. Manuf.*, vol. 61, 2023, doi: 10.1016/j.addma.2022.103316.
- [63] S. Kokare, J. P. Oliveira, and R. Godina, 'A LCA and LCC analysis of pure subtractive manufacturing, wire arc additive manufacturing, and selective laser melting approaches', *J. Manuf. Process.*, vol. 101, pp. 67–85, 2023, doi: 10.1016/j.jmapro.2023.05.102.
- [64] S. Kokare, J. P. Oliveira, and R. Godina, 'Exploring the Environmental and Economic Benefits of Wire Arc Additive Manufacturing compared to Subtractive Manufacturing', presented at the Procedia CIRP, 2024, pp. 3–8. doi: 10.1016/j.procir.2024.10.047.
- [65] P. C. Priarone, G. Campatelli, F. Montevercchi, G. Venturini, and L. Settineri, 'A modelling framework for comparing the environmental and economic performance of WAAM-based integrated manufacturing and machining', *CIRP Ann.*, vol. 68, no. 1, pp. 37–40, 2019, doi: 10.1016/j.cirp.2019.04.005.
- [66] A. Azizi and T. A. Manoharan, 'Designing a Future Value Stream Mapping to Reduce Lead Time Using SMED-A Case Study', presented at the Procedia Manufacturing, 2015, pp. 153–158. doi: 10.1016/j.promfg.2015.07.027.
- [67] 'SuperArc® G4Si1'. Accessed: Feb. 11, 2025. [Online]. Available: https://www.lincolnelectric.com/en/Products/superarcg4si1_gmaw
- [68] N. K. Gupta, G. Ganesan, S. Siddhartha, S. R. Karade, S. D. Singh, and K. P. Karunakaran, 'A Dual-Side Deposition Technique to Mitigate Deformation in Wire Arc Additive Manufacturing', *Trans. Indian Inst. Met.*, vol. 77, no. 11, pp. 3425–3434, 2024, doi: 10.1007/s12666-024-03350-8.